Norwegian University of Science and Technology
Kavli Institute for Systems Neuroscience &
Centre for Neural Computation

Intrinsic Connectivity of the Claustrum: Gap Junctions Demonstrated by Immunohistochemistry and Electron Microscopy

Master's Thesis
Faculty of Medicine, Department of Neuroscience

Supervisor: Prof. Menno P. Witter

By Peter Bennett
Trondheim, June 2014

Acknowledgments

The work presented in this thesis was performed at the Kavli Institute for Systems Neuroscience and Centre for Neural Computation at the Norwegian University of Science and Technology, under supervision of Professor Menno P. Witter.

First of all I thank Menno Witter for his excellent job as a supervisor, for all he has taught me and for preparing me for what is to come.

Much appreciation also goes to all the technicians for their support and helpful advice.

For their advice and technical support related to electron microscopy, I would like to thank Nan Tostrup Skogaker, Bruno Monterotti, Jørgen Sugar and Johannes van der Want.

Special thanks goes to Benjamin Dunn, Debora Ledergerber and Tor Stensola for interesting discussions and more importantly for making me think.

Finally, I would like to thank my parents for financial and moral support – this would not have been possible without.

Abstract

The claustrum is a much neglected nucleus in the brain, whose function remains unknown to date. Yet, based on the extensive reciprocal connections it shares with virtually all functional regions of cortex, it most likely serves a far from meaningless purpose. Current hypotheses propose a role in perceptual binding by synchronization of cortical activity. These hypotheses come with a number of assumptions, such as a wide network of connections intrinsic to the claustrum. In this context, gap junctions have been suggested as a means to interconnect portions of the claustrum and to synchronize incoming cortical activity. Neuronal gap junctions have been shown to be involved in supporting synchronous activity and oscillations in areas such as the hippocampus, making them a feasible candidate for such a mechanism in the claustrum. While gap junctions have been described in many areas of the brain, they have not been observed in the claustrum prior to the present study. Set against this background, the presence of gap junctions in the claustrum was investigated in this thesis. To this end, an immunohistochemical approach was first used to localize the gap junction protein connexin 36. Once a protocol was established, a small population of connexin 36 expressing neurons was identified in the posterior half of the dorsomedial aspect of the ventral claustrum (also known as the endopiriform nucleus). However, no further labeling was observed throughout the rest of the claustrum. These results were supported by electron microscopy, as putative gap junctions were exclusively observed in an area corresponding to where connexin 36 expression was found. These results represent the first steps in confirming the presence of the hypothesized gap junction network in the claustrum. Yet, it could be argued that their limited occurrence in both number and location are not entirely in line with current hypotheses predicting a wide gap junction network common to the entire claustrum.

Contents

Abbreviations

General:

CA1	Cornu Ammonis 1
CaBP	Calcium-binding protein
Cl	Claustrum
Cld	Dorsal claustrum
Cli	Intermediate claustrum
Clv	Ventral claustrum
Cx	Connexin
DCW	Deep cerebral white matter
DG	Dentate gyrus
EAAC1	Excitatory amino-acid transporter 1
EM	Electron microscopy
GABA	γ-aminobutyric acid
GAD	Glutamic acid decarboxylase
GJ	Gap junction
M1	Primary motor cortex
M2	Secondary motor cortex
nNOS	Neuronal nitric oxide synthase
PPC	Posterior parietal cortex
S1	Primary somatosensory cortex
S2	Secondary somatosensory cortex
SOI	Structure of interest
V1	Primary visual cortex
V2	Secondary visual cortex
Vglut2	Vesicular glutamate transporter 2

Chemicals, Tracers & Solutions:

DAB	*3,3'*-diaminobenzidine
DMSO	Cryoprotective solution
PFA	Paraformaldehyde
TBS-Tx	Cell permeablilization solution
Tris	Tris(hydroxymethyl)aminomethane

1. Introduction

1.1. What is the claustrum?

The claustrum is a thin sheet of grey matter located medial to the insular and piriform cortex and lateral to the external capsule. It is commonly subdivided into a dorsal and a ventral portion based on its morphology. The dorsal claustrum is also referred to as the insular claustrum, while the ventral claustrum is also known as the piriform claustrum or endopiriform nucleus. In rats, the claustrum stretches along the antero-posterior axis from 4.2mm in front of Bregma to 4.44mm behind (Paxinos & Watson 2007). In the dorsoventral plane it roughly follows the borders of the piriform and insular cortex. In species that have the extreme capsule, the claustrum is separated from insular cortex by this white matter tract. Nevertheless, Karl Brodmann (1909) described the claustrum as layer VIc of insular cortex – LVIb being the extreme capsule. Once the cytoarchitectonics and the projections of the claustrum were put under closer scrutiny, it became clear that it is in fact a separate entity rather than a part of insular cortex.

The claustrum has been found in all mammals studied so far (Kowiański et al. 1999; Buchanan & Johnson 2011), although it is debated whether it is present in all monotremes (Butler et al. 2002; Ashwell et al. 2004). Yet, most commonly it has been studied in cats, due to the comparatively large dorsal portion of their claustrum (figure 1; Edelstein & Denaro 2004). This has granted researchers much needed ease of access to the claustrum in both recoding and tracing studies, but has also initially led to a rather restricted view of claustral function.

The dorsocaudal claustrum in the cat is reciprocally connected with visual areas of cortex (LeVay & Sherk 1981). It is thus not surprising that an early suggestion regarding the function of the claustrum was mainly a role in visual processing (Sherk & LeVay 1983). More specifically, Sherk and LeVay (1983) proposed that the claustrum modulates the length selectivity of neurons in primary visual cortex (V1). Yet, other authors have attributed a relaying function to the claustrum and thus a similar role to that of thalamus (Spector et al. 1974). While the exact projection patterns of the claustrum are still not entirely known, the general picture of an extensive reciprocally connected network has extended the comparison between the claustrum and thalamus (Olson & Graybiel 1980). Crick and Koch (2005) have argued for a more significant role of the claustrum in proposing it to be an integrator of sensory information leading to a single unified percept. This proposal was based on the wide reciprocal connectivity between the claustrum and cortex, not only in the cat but also in most other species in which the connectivity was assessed (Olson & Graybiel 1980; Irvine & Brugge 1980; LeVay & Sherk 1981; Pearson et al. 1982; Witter et al. 1988; Zhang et al. 2001). It was further argued that the claustrum processes multimodal sensory input, based on previous studies (Segundo & Machene 1956; Spector et al. 1974; Clarey & Irvine 1986). As a final conclusion to their hypothesis, Crick and Koch (2005) have called the claustrum the most probable candidate for the neural correlate of consciousness. However, this view has been widely criticized, as several studies have failed to find direct support for it (Remedios et al. 2010; Smith et al. 2012). The definitive function of the claustrum thus remains enigmatic and promises to remain so for now, as researchers meet significant challenges in studying the claustrum.

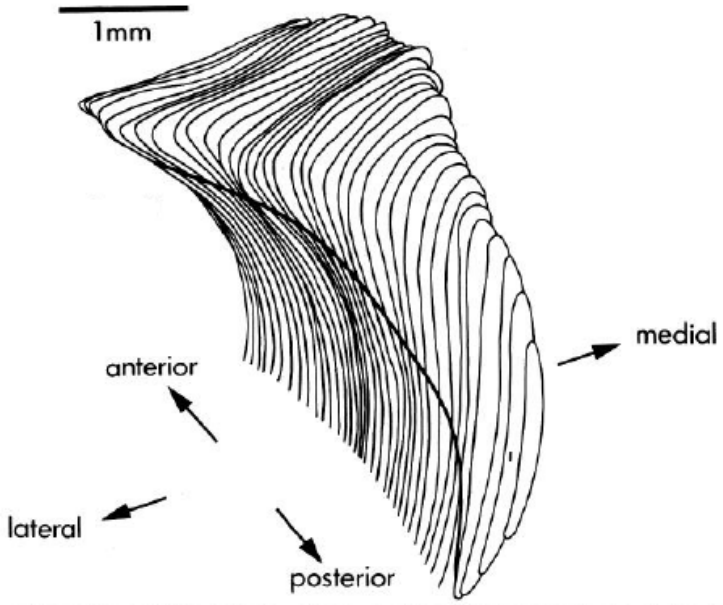

Figure 1: A 3D model of the dorsocaudal cat claustrum seen from posterolateral direction. The most rostral and ventral parts are not depicted. Modified from LeVay & Sherk (1981).

1.2. Challenges in studying the claustrum

Dedicating an entire section of this thesis to the challenges that researchers face in investigating the claustrum may seem excessive at first glance. However, it will quickly become clear that a disquisition of these challenges is warranted, as they have not only hampered the claustrum's thorough investigation but also spawned a considerable amount of debates. Most notable, discussions centered around the ontogeny, projections, exact borders and functions of the claustrum (Edelstein & Denaro 2004; Crick & Koch 2005; Mathur et al. 2009). Many of these debates remain unresolved. The lacking consensus on these subjects is at least partly attributable to the enormous difficulty in studying the claustrum and the relatively small body of research aimed at resolving these issues. In the following section, I will discuss the most striking challenges posed by the claustrum.

Definition

In the early descriptions of the claustrum by Meynert (1884) and Brodmann (1909), its borders have been only roughly described. Yet, up until recently there was a fairly clear consensus about the lateral-medial borders of the claustrum. During the last three decades of the twentieth century, researchers have agreed to put the borders of the claustrum directly adjacent to the external capsule and the insular cortex – or extreme capsule in species that poses it. However, using proteomic analysis, Mathur et al. (2009) suggested a new border of the rat claustrum based on the expression of the protein marker G-protein gamma2 subunit (Gng2). In this newly proposed definition, the claustrum is surrounded by insular cortex, rather than reaching all the way to the external capsule. Whether or not these new borders are indeed correct and universal to all species is up for debate. Nevertheless, their mere suggestion makes the complexities of studying the claustrum evident.

Morphology and comparative connectivity

The morphology of the claustrum varies substantially across different species, with distinct degrees of complexity – insectivores having the simplest and humans having the most complex (Kowiański et al. 1999). While in all species the dorsal and the ventral claustrum are recognizable, the differences between species are pronounced enough to justify a classification of at least five morphological subtypes (figure 2). Type I is found in animals such as rats and mice and is defined by the challenge in distinguishing the claustrum from neighboring cortex, as these species lack the extreme capsule. Type II – found in rabbits and guinea pigs – is differentiated from type I based on the relative ease with which cortex and claustrum can be separated, due to the presence of the extreme capsule. Type III has been described in cats and is characterized by its previously mentioned large dorsal portion. Type IV is present in non-human primates and is thinner than all other sub-types. Type V is found in humans. In this sub-type, the dorsal claustrum is split further into dorsal, temporal and orbital portions, while the ventral claustrum is divided into a paraamygdala portion and a not otherwise specified small group of neurons.

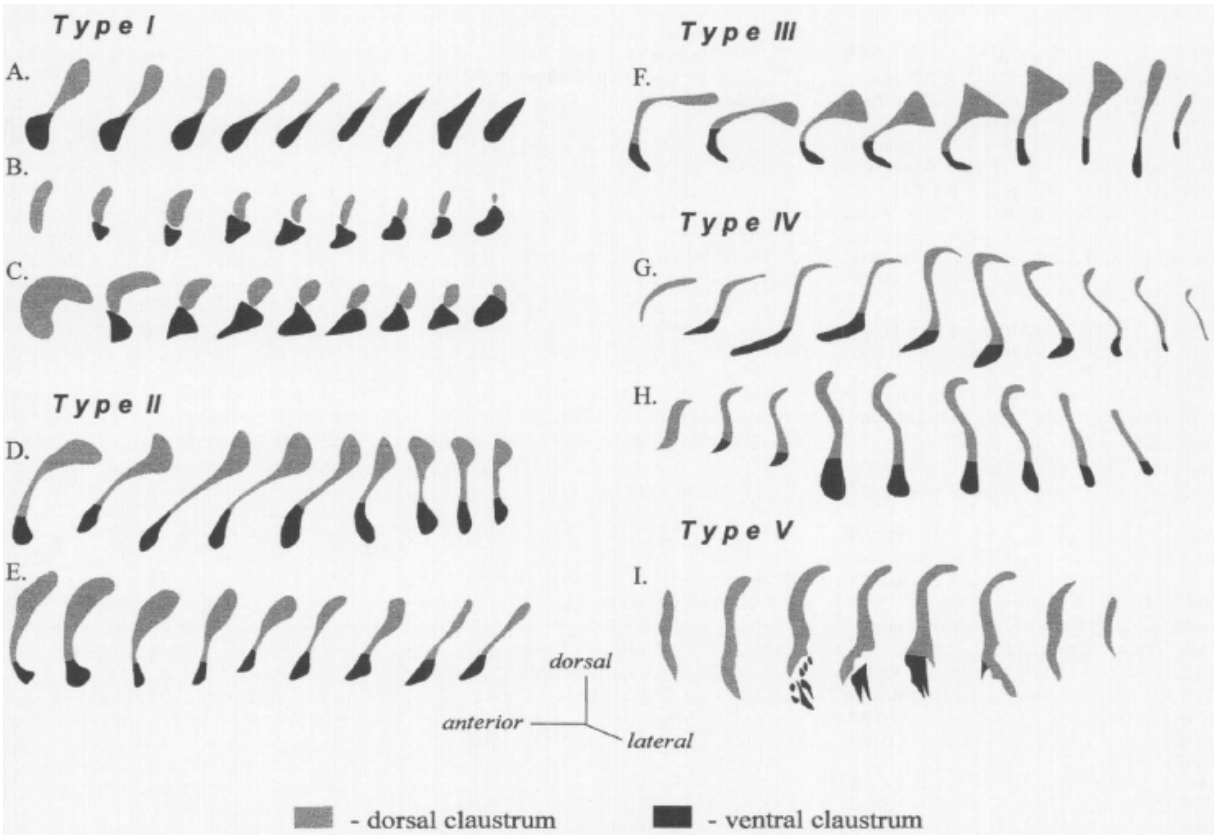

Figure 2: Schematic of coronal sections of claustral sub-types (from rostral (left) to caudal (right)). A: Sorex. B: Mouse. C: Rat. D: Guinea pig. E: Rabbit. F: Cat. G: Macaque. H: Cercopithecus. I: Human. Modified from Kowiański et al. (1999).

In addition to differences in morphology, several studies have shown species dependent distinctions in connectivity between the claustrum and other brain areas. As an example, V1 in the cat has been shown to project to the dorsocaudal claustrum (LeVay & Sherk 1981), whereas in the monkey V1 projects to more ventral portions of the claustrum (Pearson et al. 1982). When taking the morphological and connectional variations in to account, it

becomes clear that making generalizations across species regarding the claustrum – and especially its function – is far from easy.

The claustrum is a very thin structure, with the exception of the dorsal claustrum in the cat as mentioned above, thus complicating research on the claustrum. Injecting tracers directly into the claustrum generally results in leakage into adjacent structures, such as insular cortex, putamen and external capsule (e.g. LeVay & Sherk 1981; Witter et al. 1988). Consequently, the results of these studies are not always straightforwardly interpretable. Most of the knowledge on claustral connectivity is thus based on injections of both anterograde and retrograde tracers into other brain areas (Olson & Graybiel 1980; Irvine & Brugge 1980; Pearson et al. 1982; Sadowski et al. 1997). While these studies provide an insight into the topographic arrangement of claustral afferents, they give little information on the cortical layer specificity of claustro-cortical connections.

Much like the research on claustral connectivity, lesion studies also face the same challenge posed by the shape of the claustrum. Edelstein and Denaro (2004) reviewed several studies attempting to investigate the consequences lesioning the claustrum. While these studies proposed that the claustrum may be engaged in many different functions, none of the studies actually managed to produce lesions that were fully confined to the claustrum. This not only casts doubt on the accuracy of the interpretations of their results, but also further illustrates the immense difficulties found in researching the claustrum.

With regard to the challenges posed by the claustrum, its name – meaning *enclosed space* – seems most suitable. Although, knowledge on the claustrum is still limited and the results from existing studies are debatable, that what is known should not be underestimated, as it clearly suggests a significant role for the claustrum in the brain. This significance will become clearer with the descriptions of claustral anatomy and connectivity in the following sections.

1.3. Anatomy of the claustrum

1.3.1. Dorsal and ventral claustrum - a single structure?

Considering the literature on the claustrum, there is disagreement about whether the claustrum and endopiriform nucleus form a single entity or should be regarded as separate parts of the brain. Many studies focus on either the claustrum or endopiriform nucleus, while either ignoring the respective other or treating them as separate (e.g. Behan & Haberly 1999; Wójcik et al. 2004; Mathur et al. 2009). However, there is considerable amount of support for several arguments as to why the claustrum and endopiriform nucleus should be regarded as part of the same structure. Thus, in the following discussion – and throughout the entire thesis – the two parts will be referred to as dorsal and ventral claustrum (Cld and Clv respectively) or just claustrum (Cl) in the case of both together.

Studying the morphology of 26 different mammalian species, Buchanan and Johnson (2011) suggested the Cld and Clv were unusually distinctive in dogs and raccoons. However, they also reported that the Cld and Clv always form an uninterrupted mass of cells in all studied species. An early cat study of the Cl's cytoarchitecture described the Cld and Clv as having distinct cell types and density, thereby contributing to the notion of two separate structures (Druga 1966). Since this earlier research, cytoarchitectural studies in various species have extended the picture extensively by describing many distinctive cell types throughout

the entire Cl (LeVay & Sherk 1981; Braak & Braak 1982; Mamos et al. 1986; Shibuya & Yamamoto 1998; Wasilewska & Najdzion 2001; Hinova-Palova et al. 2007; Rahman & Baizer 2007). Even though not all studies agree with each other, the cell types described by them are never exclusively found in either portion of the Cl. Considering the findings of the studies mentioned above, a separation of the Cld and Clv into two distinct structures based on their morphology and cytoarchitecture is implausible.

A study using proteomic analysis found that the protein Gng2 was only found in the center of the Cld and not at all in the Clv, prompting the conclusion that only the core of the Cld should be regarded as the entire Cl and the Clv was to be fully excluded. By contrast, Pirone et al. (2012) found Gng2 expression in humans not only throughout the entire Cl, but also in the neighboring external and extreme capsule as well as in insular cortex. A number of other studies have also found that the expression of molecular markers in the Cl varies substantially across species (Arimatsu et al. 1999; Arimatsu et al. 2009; Miyashita et al. 2005; Pirone et al. 2012). These markers may delineate a border of some sort within a given species. However, there is no reasonable argument for why any single marker would indicate the separate nature of two structures, if not supported by further evidence – such as differences in connectivity or functions of said structure and its neighbors.

Some researchers have also attempted to distinguish the Cld and Clv from each other based on their ontogenetic origin. While the origin of the entire Cl is still a matter of debate, some researchers, arguing for a pallial derivation, have split the Cld and Clv into two separate entities. Puelles et al. (2000) proposed that the Cld is derived from the lateral pallium, whereas the Clv originates in the ventral pallium. Indeed these results make it seem plausible to separate the Cld and Clv into two entities; however, a study conducted by Reblet et al. (2002) has extended Puelles et al.'s (2000) results in that it suggested the Cld is derived from both the ventral and lateral pallia, making a clear distinction between the Cld and Clv less obvious. A further argument for a separation of the Cld and Clv has been put forward by Bayer and Altman (1991), who suggested that the two parts of the Cl not only develop during different time periods but also in distinct gradients. The Clv is reported to develop at E14-E15 with a ventromedial to dorsolateral gradient, while the Cld develops at E15-E16 with a posterior to anterior gradient. Bayer and Altman (1991) interpret these results in favor of separating the Cld and Clv, even though the results could well be interpreted to represent a developmental gradient of the entire Cl as a single entity, as no discontinuity in either timing nor gradient was observed by the authors. An obvious separation of the Cld and Clv based on their development therefore seems speculative.

When considering the connectivity of the entire Cl with the rest of the brain, it becomes even more evident why the Cld and Clv in fact need to be considered parts of the same structure (for a full disquisition of claustral connectivity see section 1.4). The Cl shares reciprocal connections with most parts of cortex, which are topographically organized within the Cl (Olson & Graybiel 1980; LeVay & Sherk 1981; Irvine & Brugge 1980; Pearson et al. 1982; Witter et al. 1988; Zhang et al. 2001). In cats this topography follows a gradient on a dorsoventral axis in which sensory and parasensory cortices connect to the most dorsal part of the Cl; limbic cortex to more ventral parts of the Cld; paralimbic cortex to both dorsal and ventral parts of the Clv; and possibly the olfactory cortex to the most ventral part of the Clv (figure 3; Witter et al. 1988). The continuous nature of this topography throughout the entire

Cl and the overlap seen between the projection zones strongly supports the argument of the Cld and Clv being a continuous structure.

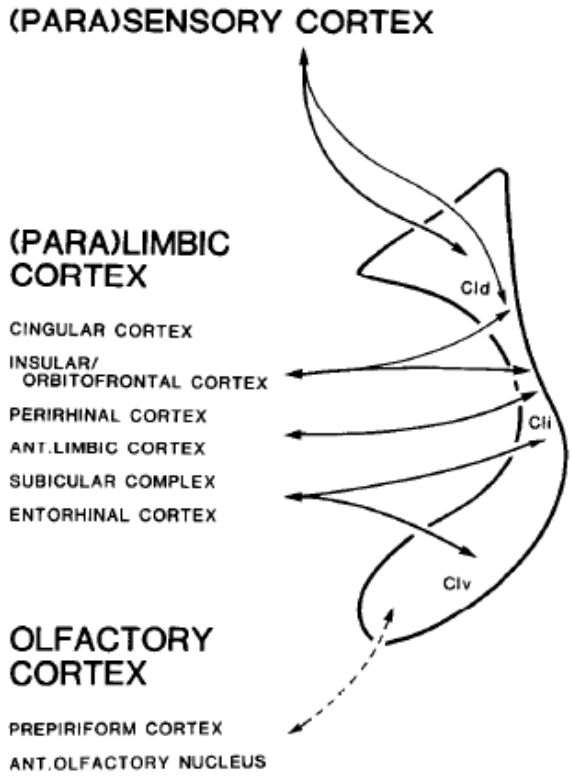

Figure 3: Schematic of afferent and efferent connections of the cat Cl with cortex. Solid lines show well established connections; dashed lines show questionable connections. Modified from Witter et al. (1988).

1.3.2. Cytoarchitecture & Cytochemistry

While the Cl has been researched in a wide variety of species, only those continuously studied – rodent, cat, monkey and human – will be discussed here in detail.

Early studies of claustral cell types relied on Golgi staining (Brand 1981; LeVay & Sherk 1981; Braak & Braak 1982; Mamos et al. 1986). Yet, the picture Golgi staining gives is often incomplete, as many distinguishing factors of cells cannot be studied using this method. However, a brief summary of the most important findings of these studies will be given in this section, as their contribution to knowledge on the Cl has nevertheless been substantial. Other attempts of classifying cell types in the Cl involved the expression of calcium-binding proteins (CaBPs), neuropeptides and markers of neurotransmitters (Celio 1990; Reynhout & Baizer 1999; Kowiański et al. 2001; Dávila et al. 2005; Real et al. 2006; Rahman & Baizer 2007; Kowiański et al. 2008; Kowiański et al. 2009; Hinova-Palova et al. 2013). While much is already known about claustral cells and their defining features, no clear consensus on their classification has been established to this point. As a result there are several different classifications for the same population of cells, which will become evident in the individual sections below.

Rodent

The Cl seems to be similar in most of its characteristics across rodent species. In this section only research using mice and rats will be reviewed, as these two species are currently the most studied rodent types.

Using intracellular staining, Shibuya and Yamamoto (1998) found cells in the rat Cl had a wide range of shapes, including polygonal, triangular, ovoid, round and fusiform. Most cells had a soma diameter of 8µm to 22µm and had three to eight primary dendrites – either spiny or aspiny. Interestingly, some of these dendrites reached into adjacent cortical areas with a path towards layer I.

The expression patterns of CaBPs (parvalbumin, calretinin and calbindin D28k) in the mouse Cl were found to be quite distinctive (Real et al. 2003). Of the three CaBPs, calbindin showed the strongest expression throughout the entire Cl. It was found in small to medium sized round, elongated and multipolar neurons, but also in some pyramidal neurons – yet the latter cell type was only observed in the Clv. Neuropil only modestly expressed calbindin. For calretinin these authors reported a rather curious expression pattern, as both cells and neuropil were observed to express calretinin throughout the entire Cl except for the core of the Cld. This pattern looks like an almost perfect inversion of the Gng2 expression in the rat (Mathur et al. 2009). Cells expressing calretinin were aspiny and had small somata of either round or bipolar shape. Additionally, parvalbumin expression in the mouse Cld was found to be fairly congruent with the calretinin-negative patch described above. In the Clv parvalbumin expression was quite irregular, with higher levels in the dorsorostral portion and lower levels at dorsocaudal and ventral portions. Parvalbumin positive cells had medium sized multipolar somata extending multiple, far reaching, beaded dendrites.

As with CaBPs, studies on γ-aminobutyric acid (GABA), neuronal nitric oxide synthase (nNOS) and vesicular glutamate transporter 2 (Vglut2) have revealed varying expression patterns in the mouse Cl (Guirado et al. 2003; Real et al. 2006). Adding to the distinctive pattern of calretinin and parvalbumin described above, it was found that the calretinin-negative core was also almost completely Vglut2-negative (Real et al. 2006). The rest of the Cld showed a gradient of Vglut2 expression – caudal and intermediate portions expressing higher levels than the rostral portion. Cells expressing nNOS in the mouse Cl can be divided into two populations: 1. Medium sized round or oval cells with no more than five primary dendrites, found across the entire Cl; 2. Small to medium sized oval or round cells, found mostly in dorsorostral and intermediate portions of the Cl and almost not at all in the Clv. While most cells of the first nNOS positive population were found to coexpress GABA, the cells of the second population hardly ever express GABA (Guirado et al. 2003).

Cat

The cat Cl has been subdivided into the common dorsal and ventral portions; yet, to aid the description of their results, Witter et al. (1988) added an intermediate portion (Cli) between the Cld and Clv, which also will be used for the purpose of this section.

As part of a series of studies focusing on various aspects of the dorsocaudal portion of the cat Cl, LeVay and Sherk (1981) described three distinct cell types (I-III) using Golgi staining. The first and most frequent type was a spiny cell reported to have a soma size ranging from 15µm to 29µm. The shape of the soma and dendrites varied from pyramidal-like cells to bi-

and multipolar cells. The second cell type were aspiny cells with much smaller cell bodies than the first type – ranging from only 10µm to 15µm. These cells had extensively branched dendrites that did not extend more than 200µm. Additionally, the axons of type II cells were observed to contact both type I and other type II cells. The third cell type reported in the study was only rarely seen and was only distinguished from type II cells by its less extensively branched, but longer reaching dendritic tree.

Also using Golgi staining, Mamos et al. (1986) reported five distinct cell types in the Cld and Cli. Yet, the only different finding between the studies of Mamos et al. (1986) and LeVay and Sherk (1981) was that the former also found larger (19-27µm) aspiny multipolar cells. However, judging by Mamos et al.'s (1986) description of the other cell types, a close resemblance to the cells described in LeVay and Sherk's (1981) study can be seen. Thus, I conclude that the Golgi studies mentioned above show very similar results, but simply interpret these in different ways. It is worth noting that whereas the study on Sherk and Levay (1981) focused on the Cld, that of Mamos et al. (1986) included the Cli as well; neither of the two studies included data on the Clv.

As with rodents, the cat Cl is quite extensively studied in terms of its cytochemistry. Not only CaBPs have been studied but also the presence of markers of neurotransmitters and second messengers.

By means of immunohistochemistry, Rahman and Baizer (2007) found parvalbumin positive cells throughout the Cl with somata of various shapes – oval, multipolar, bipolar and pear shaped – at sizes between 20µm and 30µm. Generally, these results agree with those found by Hinova-Palova et al. (2007), although these authors also found spiny parvalbumin positive cells. Based on Rahman and Baizer's (2007) study, the population of neurons that express calretinin is sparser than that expressing parvalbumin. Furthermore, the authors reported that there are only two types of cells expressing calretinin in the cat Cl. The first type of calretinin expressing cells were reported to be typical bipolar cells, similar to those described by LeVay and Sherk (1981). The second calretinin expressing cell type observed by Rahman and Baizer (2007) was described do be similar to the aspiny multipolar cells found by Mamos et al. (1986). As with the previous two CaBPs, calbindin expressing cells are always multipolar neurons found throughout the cat Cl, yet again they are less common than parvalbumin positive cells (Rahman & Baizer 2007).

Neurons expressing the excitatory amino acid transporter 1 (EAAC1), glutamic acid decarboxylase (GAD) and nNOS were found throughout the Cl (Rahman & Baizer 2007). EAAC1 was never seen to be coexpressed with any of the three CaBPs included in the study, making cells positive for both GAD and CaBPs highly probable candidates for interneurons.

Monkey

Monkey studies have used several different species, such as rhesus monkeys (*Macaca mulatta*), squirrel monkeys (*Saimiri sciureus*), macaque monkeys (*Macaca fascicularis*) or grivets (C*ercopithecus aethiops*). The majority of claustral characteristics in monkeys has been described to be generalizable across most monkey species (Brand 1981; Kowiański et al. 1999), thus no further distinctions will be assumed.

Using Golgi impregnation, Brand (1981) described three distinct cell types in the primate Cld – a large spiny neuron (type I; figure 4), a large aspiny neuron (type II) and a small

aspiny neuron (type III). Differences in the shape and size of type I neurons seemed to depend on whether they were located in a wide or narrow portion of the Cld (Brand 1981; Kowiański et al. 1999). Type I cells located in wide parts of the Cld have pyramidal bodies and a main dendrite reminiscent of apical dendrites of cortical pyramidal neurons (Brand 1981). By contrast, type I cells – located in narrow portions – have spindle shaped bodies and two main dendrites. Regardless of body shape, type I cells have very spiny dendrites reported to be longer than 500µm in some cases. Brand (1981) also commented on the significantly arborized axons that type I cells send to both the external and extreme capsule. This arborization pattern was sometimes even seen in single cells, suggesting that some type I cells project to cortical and subcortical sites simultaneously. In this context Brand (1981) also mentioned that some axons possibly terminate within the Cld; however, this may have been observed due to incomplete impregnation of the axons. Type II neurons are less abundant than type I neurons. These cells have spherical somata and up to eleven primary aspiny dendrites. Opposed to type I cells, the axons of type II cells do not seem to leave the Cld at any point. Additionally, axon arbors of type II cells were never observed to be longer than the dendrites of the same cell, indicating that these cells exclusively from local networks. The type III cells have pear-shaped somata ranging from 5.5µm to 12µm in size. These cells have three or four main dendrites that are almost completely aspiny. The axons of type III cells have many collaterals; however, none of them leave the Cld and instead they from dense plexuses that innervate a single region in the Cld.

Studying the distribution of parvalbumin, calbindin and calretinin, it was found that all three CaBPs were evenly expressed across the entire Cl (Reynhout & Baizer 1999). Most cells expressing parvalbumin were described to resemble what Brand (1981) called type II and type III. Yet, some pyramidal cells (i.e. type I in wide Cld portions) were also found to express the protein, although it was not reported whether their dendrites were spiny or not (Reynhout & Baizer 1999). Calbindin expression was mostly found in small multipolar cells (i.e. type III), yet some large multipolar (i.e. type II) and very few bipolar cells (i.e. type I in narrow Cld portions) also showed expression. By contrast to the other two CaBPs, calretinin was only found to be expressed in a single cell type – bipolar cells (i.e. type I in narrow Cld portions).

Human

Kowiański et al. (1999) suggested that the human Cl has the most complicated morphology of all species studied so far. Five different cell types in the human Cl have been described based on their morphology and their lipofuscin content using transparent Golgi staining (Braak & Braak 1982). The authors differentiated what they called type II and type V cells from type III and type IV cells based on their difference in lipofuscin content. However, lipofuscin was previously described to increase in neurons with age (Goyal 1982) and is therefore unsuitable to be used as a variable for neuron classification. Thus, the classifications made by Braak and Braak (1982) should be revised by merging type II with type III and type IV with type V resulting in only three cell types (Type I remains unchanged). Comparing these three newly suggested cell types to those described in the monkey (Brand 1981) striking similarities become apparent, where each type number resembles its respective counterpart.

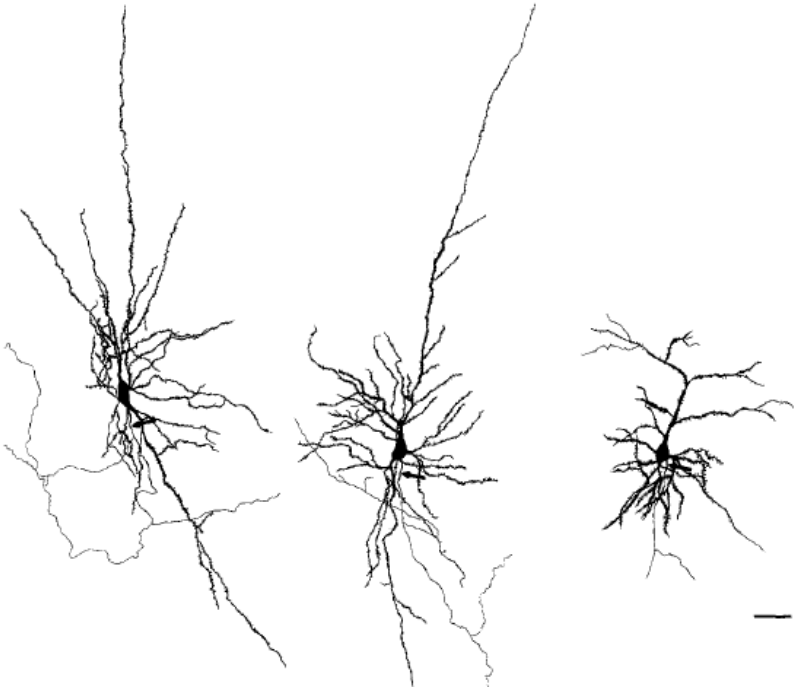

Figure 4: Golgi impregnated type I neurons in the monkey. The arrows indicate the initial segment of the axon. Scale bar: 25µm. Modified from (Brand 1981).

In terms of cytochemistry the human Cl is vastly under investigated. Research on the expression of CaBPs has focused almost exclusively on parvalbumin (Edelstein et al. 2010; Hinova-Palova et al. 2013), although there are some preliminary results on calretinin expression in the Cld (Edelstein et al. 2010). Hinova-Palova et al. (2013) found cells expressing parvalbumin for each cell type described by Braak and Braak (1982). However, the parvalbumin expressing cells were not as uniformly distributed as reported in the monkey (Reynhout & Baizer 1999; Hinova-Palova et al. 2013). Instead they were observed to be most abundant in the central wide part of the Cl, while being less expressed in the most dorsal and ventral portions of the nucleus (Hinova-Palova et al. 2013). Interestingly, the same study classified seven different cell types based on spine presence and soma size. Yet, when compared to the cells described by Braak and Braak (1982), it becomes apparent that no new cell types were found by Hinova-Palova et al. (2013), but instead the groups were subdivided into stricter defined categories.

Comparisons between species

From the studies discussed above, a few general comparisons about some claustral features and their relation to each other can be made. While Brand (1981) reported bipolar neurons only to be present in narrow portions of the monkey Cld, Reynhout and Baizer (1999) also found them distributed in wider portions of the Cl. Differences in cell populations depending on their localization in a wide or narrow portion of the Cl have also been found in the human (Braak & Braak 1982), but not in cats (LeVay & Sherk 1981; Mamos et al. 1986). This disparity may be due to species differences, although the studies by Brand (1981) and Reynhout and Baizer (1999) were both performed in monkeys. It is thus more likely that the conflicting descriptions are an indicator of the shortcomings of Golgi staining and that Brand

(1981) and Braak and Braak (1982) simply did not find the bipolar neurons present in wider Cl portions.

1.4. Connectivity of the Claustrum

Probably the most baffling feature of the Cl is the vast network it forms with both cortical and subcortical areas. It is this connectivity that has spawned the most speculation on the function of the Cl, but it is also one of its most debated features. As with the Cl's morphology, a few interspecies differences exist in terms of claustral connectivity. However, a common feature across species is the strict intrinsic topographic organization that both claustral afferent and efferent connections adhere to. A discussion of the specific similarities and differences is beyond the scope of this thesis, instead this section merely serves the purpose of illustrating the vastness of the network that the Cl is engaged in.

1.4.1. Claustral afferent projections

Projections from cortical and subcortical areas to the Cl have been studied using both anterograde and retrograde tracing methods. Several species have been used to elucidate these connections; however, only studies using rats, cats and monkeys will be discussed here, as they suffice to show the most important connections and their organization within the Cl. While only few subcortical projections to the Cl have been found, the picture emerging from studies on cortical projections shows that all functional areas project to the Cl.

Rat

By use of the anterograde tracer Phaseolus vulgaris-leucoagglutinin injected into the infralimbic and prelimbic cortex of rats, two opposing labeling patterns were found (Vertes 2004). Projections from infralimbic cortex the Cl are confined to its ventral portion, where they can be seen throughout the entire antero-posterior extent. By contrast, projections from prelimbic cortex are almost completely restricted to the Cld. Injections with the retrograde tracer Fluoro-Gold into the anterior Cld showed that the projections from prelimbic cortex originated from cortical LII and LV (Zhang et al. 2001). The same Fluoro-Gold injections labeled a vast amounts of other cortical areas. LII and LV of medial prefrontal cortex, secondary motor cortex (M2) and anterior cingulate cortex were shown to also project to the anterior Cld. Strong projections were also found from LII-IV of medial and lateral orbital cortex, while deep layers of these areas only project weakly to the anterior Cld. Further Fluoro-Gold labeled areas included parts of agranular insular cortex, primary motor cortex (M1), retrosplenial cortex, LV and LVI of parietal and secondary visual cortex (V2), LVI of V1, auditory and temporal association cortices, perirhinal cortex and the contralateral anterior Cl. Strong projections to the anterior Cld were also found from lateral entorhinal cortex, while only weak projections were seen from medial entorhinal cortex. Entorhinal cortex was also shown to project to the ventral portion of the Cld by electrophysiological recordings (Wilhite et al. 1986). While both S1 and secondary somatosensory cortex were also reported to project to the anterior Cld (Zhang et al. 2001), Smith et al. (2012) could not confirm any projections from S1; yet, confirmed the projections from M1. It has to be noted that Smith et al. (2012) used the definition of the Cl proposed by Mathur et al. (2009), meaning that the anterior Cld was not

analyzed. It is thus highly likely that Smith et al. (2012) found S1 projections to the anterior Cld, but did not include them in their results.

Not many tracing studies in rodents have focused on the Clv or subcortical areas. Those that exist found that the Clv receives projections from the anterior piriform cortex and insular cortex (Shi & Cassell 1998a; Shi & Cassell 1998b; Schwabe et al. 2004). Majak et al. (2002) described projections from different parts of the amygdala to several areas within the Cl. The lateral nucleus of the amygdala was seen to project almost exclusively to the Clv. The basal nucleus projects to the entire Cl, while the accessory basal nucleus projects mostly to the Clv but also to more caudal areas of the Cld. Sloniewski et al. (1986) described projections from thalamus to the Cl; however, considering the large and unspecific injections into the Cl, these results are highly unreliable.

Cat

Early tracing studies in the cat have revealed not only the projections from visual and somatosensory cortices to the Cld, but also their retinotopic and somatotopic (respectively) organization within the Cl (Olson & Graybiel 1980; LeVay & Sherk 1981). In the case of V1 it has also been found that the L6 pyramidal cells projecting to the Cl form a distinct population from those projecting to the lateral geniculate nucleus, thus indicating the presence of two independent visual circuits (Katz 1987). Primary and secondary auditory cortex as well as two auditory association areas located in the parietal cortex also project to the Cld, yet these projections are not tonotopically organized in the Cl (Irvine & Brugge 1980; Beneyto & Prieto 2001). Furthermore, projections from primary auditory cortex are still questionable (LeVay & Sherk 1981). Further projections to the Cld were found to arise from visual and auditory association areas located on the posterior ectosylvian gyrus (Beneyto & Prieto 2001).

Projections to the border between the Cld and Clv were described to arise from prelimbic and insular cortex, but also partly from anterior limbic cortex, perirhinal cortex and subiculum (Witter et al. 1988). However, the latter three areas also project to the Clv along with entorhinal cortex and prepiriform cortex. See figure 3 for a summary of cortical connections with the cat Cl.

Kaufman and Rosenquist (1985) described projections from the intralaminar thalamic nuclei to the Cld, where most projections arise from the central lateral and paracentral intralaminar nuclei. The anterior pretectal nuclei were also suggested to project to the Cl, yet due to highly imprecise injections these results need be taken with caution (Słoniewski 1983).

Monkey

While not many tracing studies have been conducted in monkeys, enough evidence has been found to support the statement that the vast cortico-claustral network is common to all species. Yet, all studies on the connectivity of the monkey Cl are restricted to the Cld (Roberts and Tomic's (2007) study being a possible exception), making it challenging to extend species generalizations to the monkey Clv. The dorsal portion of the Cld receives projections from both S1 and M1; yet, while the former projection is restricted to the caudal extend, the latter extends the entire antero-posterior axis of the Cld (Künzle 1975; Künzle 1977; Pearson et al. 1982). The supplementary motor area along with the dorsolateral and medial prefrontal cortex show a curious projection pattern in that they form a diagonal band from the anterior

dorsal Cld to the posterior ventral Cld (figure 5; Pearson et al. 1982). The prefrontal cortex also has been suggested to project to the Clv, however this is not entirely clear from the shown data (Roberts & Tomic 2007). The projections of visual areas (Brodmann 17 and 18) to the ventral portion of the Cld in the monkey contradict the general trend seen in other species by which sensory cortices tend to project to more dorsal portions of the Cld. Projections from the superior temporal gyrus and orbitofrontal cortex were also seen to terminate in the ventral Cld (Pearson et al. 1982). Cortical projections to the Cld in the monkey seem to follow a general rule. By this rule the projections of directly connected areas of cortex overlap within the Cld, while the projections from cortical areas that are not connected do not overlap in the Cld (Pearson et al. 1982). Authors refereeing to this rule have also called it the Pearson rule.

Using immunohistochemical methods, it was shown that the entire monkey Cld receives strong serotonergic input from both median and dorsal raphe nuclei (Baizer 2001).

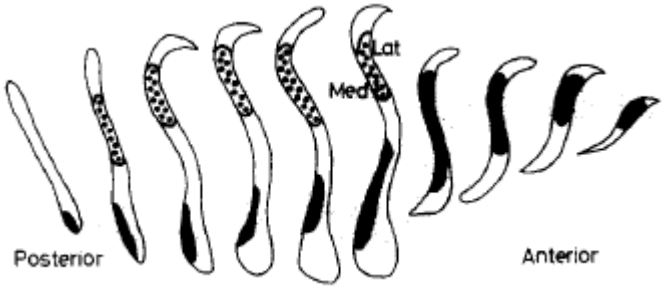

Figure 5: Projections from S1 (dotted) and from the supplementary motor area, dorsolateral and medial prefrontal cortex (solid) to the monkey Cld. Modified from Pearson et al. (1982).

1.4.2. Claustral efferent projections

Most claustral projections are reciprocal, as will become clear in the following section. Yet, not all efferent projections originate in the exact same claustral area targeted by the corresponding afferent projections. Again, as in the previous section only studies done in rats, cats and monkeys will be discussed here.

Rat

By examining the expression of vesicular glutamate transporter 2 (Vglut2) and the projection target of the neurons expressing it, Hur and Zaborszky (2005) found that the Cld was one of the main sources of glutamatergic input to neocortex. Several studies have shown the large amounts of projection targets of the Cld. Among these targeted areas are motor, somatosensory, visual and auditory cortices (Minciacchi et al. 1985; Sadowski et al. 1997; Zhang et al. 2001; Colechio & Alloway 2009). Additionally, it has been suggested that the areas in the Cl projecting to visual and auditory cortices overlap with each other, as well as those projecting to motor and somatosensory cortices (Sadowski et al. 1997). Furthermore, Smith et al. (2012), showed that in some cases single claustral neurons project to both M1 and S1. Additional projections from Cld target posterior parietal cortex (PPC), perirhinal cortex, lateral entorhinal cortex, anterior insular cortex, piriform cortex, orbitofrontal cortex, medial agranular prefrontal cortex, cingulate cortex, infralimbic and prelimbic cortices and retrosplenial cortex (Minciacchi et al. 1985; Majak et al. 2000; Zhang et al. 2001; Hoover & Vertes 2007).

The Cld also projects to a number of subcortical regions. These include thalamic midline nuclei, olfactory nucleus, olfactory tubercule, shell of nucleus accumbens, bed nucleus of stria terminalis, ventral pallidum, amygdala, hypothalamus, substantia nigra, periaqueductal grey and dorsal raphe nucleus (Zhang et al. 2001; McKenna & Vertes 2004). It has also been suggested that the posterior thalamic and pretectal region get inputs from the Cld; however, these results are based on highly unspecific injections and are thus deemed unreliable (Sloniewski et al. 1985).

The projections of the Clv in the rat have not nearly been studied as extensively as those of the Cld. The studies that exist have found projections from the Clv to piriform cortex, perirhinal cortex, entorhinal cortex, agranular insular cortex, orbital cortex, prelimbic cortex and infralimbic cortex (Behan & Haberly 1999; Hoover & Vertes 2007). Subcortical areas receiving projections originating from the Clv include the amygdala, olfactory nucleus and olfactory tubercule (Behan & Haberly 1999).

Cat

Efferent projections of the cat Cl have not been as well described as those in the rat, yet a number of studies exist that show a similarly extensive connectivity. The Cld in the cat projects to visual areas including V1, V2 and higher order areas in the inferior temporal gyrus (Olson & Graybiel 1980; LeVay & Sherk 1981; Kuchiiwa et al. 1984; Kuchiiwa et al. 1985; LeVay 1986; Jakubowska-Sadowska et al. 1998). Other areas that receive projections from the Cld are the parietal association cortex, somatosensory cortex and pericruciate cortex (Irvine & Brugge 1980; Olson & Graybiel 1980; Minciacchi et al. 1985; Jakubowska-Sadowska et al. 1998). Primary auditory cortex also has been reported to receive projections from the Cld (Neal et al. 1986); however, this was not supported by Olson and Graybiel (1980).

The area around the border between the Cld and Clv has been suggested to project to the anterior limbic cortex and perirhinal cortex. More ventral areas of the Cl but partly also the border area projects to the subicular complex and the entorhinal cortex. Piriform cortex and the anterior olfactory nucleus have also been suggested to receive projections, although these results are not entirely clear (Witter et al. 1988).

Monkey

All the afferent projections reported by Pearson et al. (1982) mentioned in the previous section were suggested to be reciprocated from the exact same claustral areas by the same authors. This means that S1 receives projections from the dorsal portion of the Cld, which also has been reported to be somatotopically organized (Minciacchi et al. 1991). Furthermore, the diagonal band from the anterior dorsal Cld to the posterior ventral Cld projects back to the supplementary motor area and the dorsolateral and medial prefrontal cortex (Pearson et al. 1982; Roberts & Tomic 2007). The medial PPC receives projections from the border area of the Cld and Clv (Leichnetz 2001). The prefrontal cortex has been proposed to receive projections from the entire Cl, although this is not clearly indicated (Roberts & Tomic 2007). Several motor areas have also been described to receive input from the entire Cld (Tanne-Gariepy et al. 2002). The ventral Cld of the monkey also projects to several visual areas, including V1, V2 and MT (Pearson et al. 1982; Lysakowski et al. 1988; Weller et al. 2002). Other areas receiving projections from the ventral Cld include the superior temporal gyrus and the

orbitofrontal cortex (Pearson et al. 1982; Roberts & Tomic 2007). The Cld also projects to subcortical areas, namely the lateral dorsomedial thalamus (Erickson et al. 2004).

1.4.3. Intrinsic projections

The intrinsic connectivity of the Cl – especially between the Clv and Cld – is still only partially known. An early study argued that no connections between different areas of the Cl were present; however, it was also acknowledged that the methods used were not entirely adequate to show internal connections (LeVay & Sherk 1981). By contrast, a few later studies have found some support for the presence of intrinsic connections. Through injection of glutamate into the Cld it was possible to record epileptiform excitatory postsynaptic potentials in the Clv, thus giving an indication of possible connectivity between the two portions (Hoffman & Haberly 1993). Based on tracer injections into either portion of the Cl, Behan and Haberly (1999) reported sparse reciprocal projections between the Clv and Cld, but also abundant far-reaching projections within each portion. Nevertheless, the injection sites of the latter study seemed slightly too big to be able to make the described conclusions. Additional support for intrinsic connectivity was given by Zhang et al. (2001), who injected both Phaseolus vulgaris-leucoagglutinin and fluoro-gold into the anterior Cl. The authors reported sparse connections from the Cld to the dorsal part of the Clv, but these were not reciprocated and thus partly contradict the results by Behan and Haberly (1999). Based on the description in the monkey of cell types whose axons do not leave the Cl (Brand 1981), connections intrinsic to the Cl could be inferred. Although it has to be kept in mind that this description was based on Golgi staining and thus it is possible that axons were not fully stained.

The studies discussed above give a far from clear picture of the intrinsic claustral connectivity. Interestingly newer hypotheses of claustral function rely quite heavily on a wide intraclaustral network, thus allocating high priority to the resolution of this particular issue (Crick & Koch 2005; Smythies et al. 2014).

1.5. Hypotheses of claustral function

Surely the most debated aspect of the Cl is its function. Many suggestions have been put forward, but none have been experimentally supported sufficiently so far. During the earlier years of research on the Cl only few authors speculated on claustral function. In 2005 Crick and Koch published a new hypothesis, thus inspiring more research and hypotheses on the topic. Therefore the present discussion on the potential function of the Cl will be divided into three sections: (1) Pre-Crick and Koch; (2) Crick and Koch's hypothesis; (3) Post-Crick and Koch.

1.5.1. Hypotheses of claustral function – Pre-Crick and Koch

Early studies on the Cl largely focused on its vast connectivity and thus speculations on the Cl's function were mostly based on this factor. It is therefore not surprising that comparisons between claustral and thalamic connectivity led to speculations that the Cl and thalamus may have similar functions. However, in this context it was also noted that the Cl does not receive direct input from ascending sensory pathways and thus was termed a "satellite" of neocortex rather than a sensory relay (Olson & Graybiel 1980).

A more specific suggestion of how the Cl may contribute to cortical processing was put forward by Sherk and LeVay (1983). The authors produced lesions in the dorsocaudal cat Cl by injecting kainic acid and proceeded to characterize the changes in receptive fields of neurons in V1. Reduced – yet not abolished – end-stopping was observed, thus prompting the conclusion that the Cl may take part in modulating receptive field properties in visual areas. While this suggestion was limited to a single sensory process, the possible modulatory effects might be applicable to all the areas the Cl is connected to.

Other proposals of claustral function have been related to the claustral-entorhinal-hippocampal network. Both Wilhite et al. (1986) and Witter et al. (1988) suggested the Cl may have a relaying function between higher-order cortices and the parahippocampal area, which in turn sends information on to the hippocampus. Since the latter structure has been shown to be involved in memory processing, it has been suggested that the Cl may play an integral part in in this system by transferring multisensory information to the parahippocampal area.

Later studies argued for an involvement of the Cl in cross-modal processing. Ettlinger and Wilson (1990) proposed that the Cl – specifically its ventral portion – provides a pathway for different areas of the brain to access each other directly. It is the authors' opinion that such a pathway would eliminate the need for a 'hub' of multimodal information in which such information would be processed and stored. Hadjikhani and Roland (1998) agree with this hypothesis based on their positron emission tomography study in which they found activation of the insula-claustrum region during multimodal tasks.

1.5.2. Hypothesis of claustral function - Crick and Koch

The main reason why Crick and Koch's (2005) hypothesis on what the function of the Cl may be warrants its own section is the huge impact it had on research focusing on the Cl. Furthermore, it seems to be the first attempt of a more detailed hypothesis, as previous authors have merely given vague speculations.

In his quest to find the neural correlate of consciousness, Crick agreed with several other researchers that it must comprise a mechanism that quickly integrates several unimodal inputs to create a single unified percept. Taking the vast network into account that the Cl is involved in, Crick and Koch suggested that the Cl was an ideal candidate for the neural correlate of consciousness. However, the authors also realized that their hypothesis comes with a number of assumptions and requirements. One of these requirements would be a coincidence detection mechanism within the Cl that would enable high temporal precision during sensory binding. Yet, inputs to the Cl that need to be bound would need to arrive synchronously in order to trigger the coincidence detector. Crick and Koch suggested that the Cl could impose such synchrony on the structures it is connected to, thereby assuming the role of what the authors call the "conductor" of the brain. Nevertheless, as Crick and Koch themselves noted, in order to produce synchrony within the Cl that could be propagated to other areas of the brain, the Cl would require certain anatomical features fit for such a task. As part of their hypothesis, Crick and Koch propose four alternatives of anatomical features that the Cl may have permiting it to produce synchrony and thus perform sensory binding: (1) widely extending axons of afferent projections; (2) an interneuron type with far reaching processes; (3) Dendro-dendritic chemical synapses; (4) a network of interneurons connected by gap junctions (GJs). While acknowledging all four possibilities as feasible, Crick and Koch

commented on how GJs would be the most probable, as they have been associated with synchronizing local networks of interneurons (see section 1.6 for further details).

The great impact that Crick and Koch's paper had can be seen by the sudden increase of studies focusing on the Cl after 2005. As it is beyond the scope of this thesis to address all the studies influenced by Crick and Koch's hypothesis, only two examples will be discussed here briefly to illustrate the significance of Crick and Koch's hypothesis.

Remedios et al. (2010) recorded the responses of claustral neurons of alert monkeys, during the presentation of audio-visual stimuli. The aim of the study was to find neurons responding to both auditory and visual stimuli, thus supporting the argument that the Cl possibly integrates several unimodal inputs into a single multimodal signal. However, only a minority of recorded neurons produced the expected responses and thus Remedios et al. (2010) concluded that they could not support the hypothesis by Crick and Koch. In contrast, Stiefel et al. (2014) argued in favor Crick and Koch's proposition of the Cl's involvement in consciousness. Firstly, these authors noted the unusually high quantity of κ-opioid receptors in the Cl. Based on this, they argued that the agonist of these receptors – salvinorin A (the active ingredient of the drug *Salvia divinorum*) predominantly acts on the Cl. This interaction was suggested to explain the consciousness-altering effects of *Salvia divinorum* reported by its users and thus proposed to support the role of the Cl in consciousness.

1.5.3. Hypothesis of claustral function - post-Crick and Koch

Most of the studies involving the Cl that have been published since 2005 have related their findings to Crick and Koch's hypothesis in one way or another. However, not only experimental work was inspired by their hypothesis, but also further theoretical ideas. In 2012, Smythies, Edelstein and Ramachandran published their first paper on a hypothesis of claustral function, that has been revised several times since then (Smythies et al. 2012a; Smythies et al. 2012b; Smythies et al. 2014). Their hypothesis shares many aspects with that of Crick and Koch and while some more detailed suggestions were made, the vast majority of these suggestions are highly speculative. Similar to Crick and Koch's suggestion, Smythies et al. (2014) propose that the Cl essentially operates as a synchronizer of cortical activity, thus leading to binding of sensory information and eventually consciousness. It is added that the Cl may have a role in motor, cognitive and salience processes. A key intraclaustral mechanism that is continuously mentioned throughout the hypothesis is the Cl's capacity to produce and amplify oscillations internally and to propagate them to different cortical areas. Interestingly, Smythies et al. (2014) described GJ linked interneuron networks as pivotal in achieving all suggested oscillation related mechanisms intrinsic to the Cl. Thus both the newest (Smythies et al. 2014) and the most influential hypothesis (Crick & Koch 2005) of claustral function rely substantially on the presence of GJs in the Cl. In the next section I will therefore discuss GJs in further detail, in order to elucidate the relevance they may have for claustral function.

1.6. Neuronal gap junctions - Structure, physiology and functions

GJs are channels between adjacent cells, providing rapid exchange of metabolites and electrical current. In mammals, they are formed by two hemichannels, called connexons with each connexon comprising six membrane-spanning proteins, called connexins (Cx; figure 6). In the brain several different cell types (i.e. astrocytes, oligodendrocytes and neurons) are

known to be connected by GJs (Connors & Long 2004); however, only those connecting neurons will be discussed here.

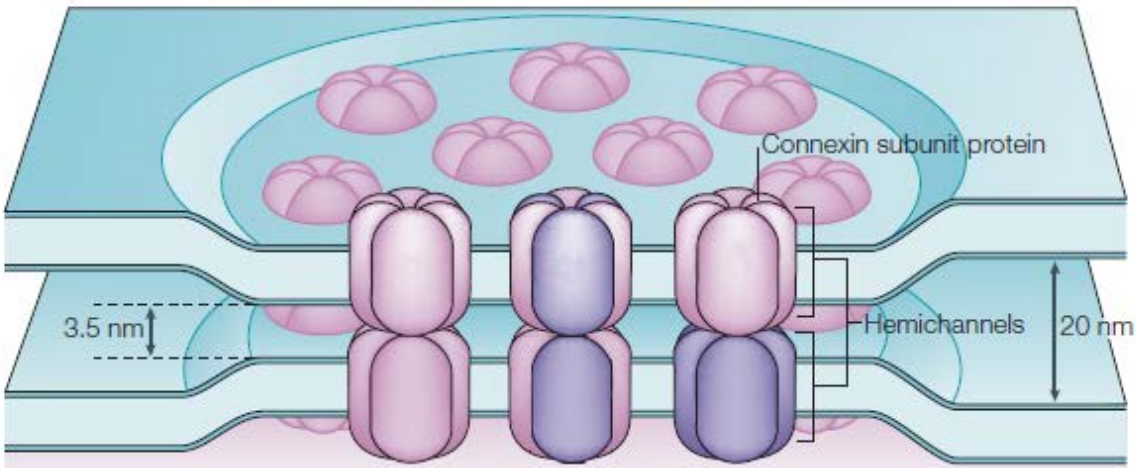

Figure 6: Schematic of GJ structure. Modified from Söhl et al. (2005)

While GJs are likely permeable to molecules of up to 1kDa, their exact physiological properties are dependent on the Cx-type they are formed by. Neuronal GJs can be composed of three Cx-subtypes – Cx36, Cx45 and Cx57 (Söhl et al. 2005). Being the most common neuronal type, Cx36 GJs seem to differ substantially from other Cx-type GJs in several characteristics. The main state conductance of Cx36 GJs was found to be only 10-15pS (Srinivas et al. 1999), while that of Cx45 GJs was found to be more than double at around 32pS (Bukauskas et al. 2002). However, GJ-conductance is dependent on intracellular pH. Cx36 GJs have been found to reduce their conductance in an alkaline environment, thus contrasting other Cx-type GJs that reduce their conductance in an acidic environment (González-Nieto et al. 2008).

The presence of GJs can be investigated by a number of different approaches. The localization of Cxs using immunohistochemistry or their mRNA using *in situ* hybridization has been quite successful. Nevertheless, these methods only give an indication of the presence of GJs, since they do not confirm their actual functionality. Combining these methods with single cell dye injections, electrophysiological recording or electron microscopy (EM) can conclusively confirm the presence of GJs. By use of the mentioned methods, most parts of the brain have been investigated for the possible expression of GJs. Cortical and subcortical pyramidal cells and interneurons both have been found to form GJs on almost various parts of the cell (Schmitz et al. 2001; Fukuda et al. 2006; Wang et al. 2010). Cx36 GJs have been found to be most abundantly expressed in the inferior olive, retina, olfactory bulb, CA1, CA3 and hilus of dentate gyrus in the hippocampus, although other areas express this type as well but in lower concentrations/densities (Schmitz et al. 2001; Hormuzdi et al. 2004). Cx45 GJ expression is not nearly as well researched, yet it was described in the striatum, cerebellum, hippocampus and most of thalamus (Maxeiner et al. 2003). At this point it should be noted that the expression of GJs is generally much higher throughout the brain during development reaching peak levels at around P16 and adult-like levels at around P24 (Belluardo et al. 2000; Maxeiner et al. 2003).

GJs have been described to be involved in developmental processes (Sutor & Hagerty 2005), regulation of intracellular ATP (Schock et al. 2008) as well as various functions related to network synchronization and oscillations (Deans et al. 2001; Traub et al. 2003; Vervaeke et al. 2010). Deans et al. (2001) showed the involvement of GJs in synchronizing neocortical interneuron networks. Recordings from L4 barrel cortex of Cx36 knock-out mice showed that firing synchrony between low-threshold spiking interneurons was markedly reduced compared to wild type animals. However, network synchrony was not completely abolished. Similar results were obtained by Hormuzdi et al. (2001), who showed that Cx36 knock-out mice had impaired gamma oscillations in hippocampus, but retained ripple activity.

A computer-simulated network of pyramidal and interneurons linked through GJs was used to show that axo-axonal GJs between pyramidal neurons alone were sufficient to produce oscillations (Traub et al. 2003). However, differences in network dynamics were observed dependent on the cell type that was GJ-coupled. While GJ-coupled principle cells are associated with oscillations at around 200 Hz (Draguhn et al. 1998), GJ-coupled interneurons are related to gamma oscillation (Traub et al. 2001). Furthermore, it was shown that synchronous firing of Cx36 GJ-coupled interneurons is highly dependent on the timing of the input that they receive (Vervaeke et al. 2010). Stimulations given in phase with the network oscillations did not disrupt synchronous firing. However, single or short burst stimulations out of phase caused interneurons to inhibit their neighboring neurons via GJs thereby causing a phase delay and a desynchronization of the network. Although the latter authors discussed the implications of their results, they did not mention the possibility that the network dynamics they described could be the underlying mechanism of a coincidence detector, as synchrony only prevailed with phase-coincident input.

1.7. Aim

Several aspects of the Cl remain debated, only partially described or simply unknown. One of these aspects is its intrinsic connectivity. As discussed above, the existing studies on this issue give a far from complete picture and indications of an intrinsic network remain questionable. Despite this, current hypothesis on claustral function rely heavily on the presence of an intrinsic network. More specifically a network of GJs throughout the Cl is assumed to fulfill the task of synchronizing input to the Cl. In areas such as hippocampus, GJs have been suggested to contribute to oscillations; thus if GJs are in fact present in the Cl, they could indeed fulfill the proposed role. However, to date no conclusive account has been given on whether GJs exist in the Cl. The aim of the present thesis is therefore to investigate the occurrence of GJs in the Cl.

2. Methods

Several protocols for perfusions, tissue sectioning, immunohistochemistry and tissue preparation for EM were tested to obtain optimal results. Final protocols are described in the present section, whereas other tests along with their results will be explained in the results section (section 3.). All detailed protocols and recipes of used solutions can be found in appendix III and IV respectively. A list of chemicals, antibodies and their manufacturers are given in appendix V.

2.1. Animals

In total ten adult Sprague Dawley rats and two in-house bred GAD67-eGFP positive adult mice were used in this study. Eight rats and one mouse were used for immunohistochemistry. Two rats and one mouse were used for EM. All rats were ordered from Charles River, Germany. Animals were treated in accordance with the regulations given by the Norwegian Animal Research Authority (NARA).

2.2. Perfusion and tissue sectioning

Perfusion and tissue sectioning protocols differed in a number of variables depending on whether the tissue was used for electron EM or immunohistochemistry. However, for both types of perfusions animals were anaesthetized with 2.5ml Isoflurane and 1ml/1kg Pentobarbital. Absence of reflexes was used as indication that animals were completely anaesthetized.

Immunohistochemistry

For immunohistochemistry, animals were first transcardially perfused with 4°C cold ringer solution and then with 4°C cold 4% paraformaldehyde (PFA) in 125mM phosphate buffer. Brains were removed from the skull and immediately put into 4°C cold phosphate buffer containing 2% dimethyl sulphoxide and 20% glycerin (DMSO) for cryoprotection. Tissue was kept in DMSO at 4°C for 48 hours before sectioning.

Cutting was performed using a sliding microtome (Microm HM430, Thermo Scientific, Waltham, USA) in conjunction with a cooling system (Microm KS34S, Microm international, Walldorf, Germany). With the caudal side down, brains were mounted with a 30% sucrose solution and kept at a temperature of around -40°C with the help of pulverized dry ice (frozen carbon dioxide). Coronal sections were cut at 20µm and separated into 6 equally spaced series. Each series therefore comprised sections with 100µm spacing. All series were stored in DMSO at -20°C until immunohistochemical processing.

Electron microscopy

For EM, animals were perfused transcardially with 4°C cold ringer solution and subsequently with 125mM phosphate buffer containing 4% PFA and 0.3% glutaraldehyde. Brains were removed from the skull and stored in 2% glutaraldehyde in 125mM phosphate buffer for 1 hour before being sectioned.

Tissue was cut horizontally at 50µm with a vibrating microtome (Leica VT1000S, Leica Biosystems, Nussloch, Germany) in a 4°C cold 125mM phosphate buffer bath. Sections were

cut into smaller pieces containing the Cl and surrounding areas before being processed for EM.

2.3. Immunohistochemistry: Connexin 36

First, the sectioned tissue was washed in 125mM phosphate buffer. Secondly, the sections were washed in Tris-buffered saline containing 0.5% Triton X-100 (TBS-Tx) to permeabilize cell membranes. In order to prevent unspecific staining, unspecific binding sites were blocked by washing the tissue in TBS-Tx and 5% normal goat serum. Following these steps, the tissue was incubated in primary antibody (mouse anti-connexin 36; Invitrogen, Ltd., Paisley, UK) diluted at 1:500 in TBS-Tx for 24 hours at 4°C. After incubation with primary antibody, the sections were rinsed in TBS-Tx and incubated for 90 minutes at room temperature in secondary antibody (Alexa Fluor 488 goat anti-mouse; Invitrogen, Ltd., Paisley, UK) diluted at 1:400 in TBS-Tx. The tissue was then rinsed in Tris-HCl buffered solution, mounted on microscope slides (Menzel glass slide, Gerhard Menzel GmbH, Braunschweig, Germany) from Tris-HCl buffered solution containing 0.2% gelatin. Mounted sections were dried for a minimum of 12 hours, then cleared in a toluene bath and finally coverslipped with the toluene containing mounting medium entellan.

2.4. Tissue preparation for electron microscopy

Sections were first washed in cacodylate buffer and subsequently post-fixed with 1% Osmiumtetroxide and 1,5% potassium ferrocyanide in cacodylate buffer. The tissue was then washed in cacodylate buffer again and subsequently dehydrated with ethanol. Dehydrated sections were flat-embedded in propyleneoxide and epoxy between two sheets of clear plastic foil. Tissue was stored in 60˚C overnight to allow for polymerization of the epoxy. Pieces of Cl were then cut from the flat-embedded tissue and glued to epoxy-blocks. Epoxy-blocks with the attached tissue were left to harden in 60˚C for 48-72 hours. Ultrathin sections were cut on an ultramicrotome (EM UC6, Leica Microsystems, Wetzlar, Germany) at 40-60nm. Tissue was collected on mesh-grids and stained with uranyl acetate and lead citrate.

2.5. Analysis

Sections processed for immunohistochemistry were analyzed with a fluorescent microscope (Axio Imager M1, Carl Zeiss MicroImaging, Jena, Germany) and a confocal microscope (LSM 510, Carl Zeiss MicroImaging, Jena, Germany). EM tissue was analyzed with a transmission electron microscope (JEM-1011, JEOL ltd., Tokyo, Japan). Electron micrographs were taken with and processes with iTEM (Olympus Soft Imaging Solutions GmbH, Münster, Germany).

3. Results

3.1. Immunohistochemistry

3.1.1. Connexin 36 antibody tests

Several tests for Cx36 labeling had to be performed – initially to overcome a set of problems such as auto-fluorescence and eventually to obtain a strong and specific signal. In order to achieve optimal staining, numerous perfusion and incubation protocols were tested. See table 1 for a summary of manipulated variables and the values used in the final protocol. Images of all tests can be found in appendix I.

Table 1: Summary of all variables changed during tests, with their tested and final values.

Variable	Tested	Used for final protocol
Ringer (ml)	250; 100; 50; 25	25
PFA (ml)	250; 100; 80	100
PB Rinse (ml)	80; 50; no	No
Post-fixation (h)	24; 20; no	No
Section thickness (µm)	40; 20; 10	20
Primary antibody type (host / clonality)	Rabbit - Polyclonal; Mouse - Monoclonal	Mouse - Monoclonal
Secondary antibody (Conjugate)	Alexa 488; Alexa 546; Cy3	Alexa 488
Primary antibody incubation time (h)	16; 24; 48	24
Primary antibody dilution (Antibody : Buffer)	1:250; 1:500; 1;1000	1:500
Blocking agent	Normal Goat Serum; No	Normal goat serum
Cell permeabilization agent	TBS-Tx (0.5%); Saponin (0.1/0.4%)	TBS-Tx (0.5%)
Species	Rat; Mouse	Rat

For the following tests, I used a polyclonal rabbit anti-connexin 36 antibody (Invitrogen, Ltd., Paisley, UK) unless otherwise specified. Case 18296 showed strong auto-fluorescence (Appendix I, figure I A), which was eliminated by reducing the volume of both the ringer and fixing solutions used during perfusions. Once this was established, the primary antibody dilution was set at 1:500 and incubation time at 16 hours based on Rash et al.'s (2000) study, which used the same primary antibody. However, under these conditions no signal could be found in areas where presence of Cx36 has been previously described (see introduction for a review), as for example in hippocampal CA1 (Appendix I, figure I B). Subsequently, using tissue from the same animal, both longer incubation times (24 hours and 48 hours) and a higher concentration of primary antibody (1:250) were tested in separate experiments. In all tests, expected areas only showed weak labeling with strong background staining (Appendix I, figure II A, C & E). Furthermore, strong and highly abundant labeling was also seen in neocortical pyramidal cells including their apical dendrites (Appendix I, figure II B, D & F). As pyramidal cells in neocortex have not been described to express Cx36 to this degree, this labeling was dismissed as unspecific – a suspicion supported by later tests in which pyramidal cell labeling was absent while expected labeling remained.

In order to rule out that the secondary antibody was causing the unspecific labeling, a Cy3 conjugated antibody raised in donkey was used in the next test. While the expected signal remained similar to previous tests, unspecific labeling in neocortex was increased (Appendix I, figure III A & B). Thus, the previously used alexa 488 conjugated secondary antibody was continued to be used in subsequent tests.

A blocking step with normal goat serum for one hour was added to the next test to decrease background and unspecific staining. While specific labeling remained similarly weak, unspecific labeling was slightly decreased (Appendix I, figure III C & D). Therefore blocking was added to the standard protocol.

In an effort to increase the signal of the specific labeling, tissue sections were heated to approximately 60°C for two hours before the first buffer wash. Heating has been suggested to split protein cross-links caused by fixative and therefore reveal more antigens (Shi et al. 2011). However, this method drastically reduces the quality of the tissue, making the tissue incredibly fragile. While the specific labeling in this test was slightly stronger, the background and unspecific staining was also increased (Appendix I, figure III E & F). As the results of this test did not make up for the decreased tissue quality, heating was not included into the standard protocol.

Since tissue heating was deemed insufficient to resolve potential fixative induced protein cross-linking issues, two new perfusion protocols were tested. For the first protocol, the animal was perfused with less ringer solution in order to decrease the time taken until fixation and thus fix the tissue in a more healthy state. Additionally, the animal was perfused with only 80ml of PFA followed by perfusion with approximately 80ml of phosphate buffer to rinse out the PFA. Additionally, the brain was not post-fixed, but put into DMSO immediately after being removed from the skull. However, the brain proved to be insufficiently fixed and thus sectioned tissue dissolved during the first few buffer washes. The second protocol was identical to the first with the exception of using 100ml of PFA and 50ml of phosphate buffer. Tests with this brain showed reduced background and unspecific staining in neocortex, while the previously observed specific labeling was maintained (Appendix I, figure IV A & B).

To reduce the unspecific staining even further, 5% goat serum was added to the primary antibody solution. However, while unspecific staining was reduced, specific labeling was also reduced (Appendix I, figure IV C & D). Blocking was thus kept as a separate step before incubation with the primary antibody.

A further test was performed on tissue sectioned at 10µm with the aim of increasing visibility of the weak specific signal – previously tissue was sectioned at 40µm. The thicker the tissue the more light – needed to excite the fluorophores – but also the light emitted by the fluorophores will be absorbed by the tissue. Unfortunately, the tissue cut at 10µm proved to be too fragile and dissolved before any tests could be completed. New tests with tissue cut at 20µm were more successful. Although the specific signal remained weak, background staining was significantly reduced (Appendix I, figure IV E & F). I therefore decided to cut tissue at 20µm.

As Cx36 is a membrane protein, there is the possibility that triton was too strong as a permeabilization agent and may remove the protein along with parts of the membrane, explaining the weak specific signal. Yet, since the primary antibody is against the cytoplasmic loop domain of Cx36, cell permeabilization is necessary. Therefore, I performed tests with

saponin – a detergent selectively removing cholesterol – at concentrations of 0.1% and 0.4% (Appendix I, figure V A-D). No difference between saponin permeabilization and previous tests could be observed, thus triton was continued to be used.

Unspecific staining remained an issue to this point. Tests using a GAD67-eGFP positive mouse was therefore performed. Firstly to check for a potential species effect, but also to check for Cx36-GAD67 colocalization in case the test worked. Cx36-GAD67 colocalization would indicate that Cx36 positive neurons are GABAergic (i.e. putative interneurons), having implications on the GJ-network dynamics (as discussed in section 1.6). For this test two series from horizontally sectioned brain were used. Tests with a primary antibody dilution of 1:1000, using an alexa 546 conjugated secondary antibody revealed almost no labeling (Appendix I, figure VI C & D). At a dilution of 1:500 the unspecific labeling in neocortex almost disappeared, while specific labeling was even weaker than in previous tests using rats (Appendix I, figure VI A & B). Therefore, rats were continued to be used.

Following the lack of success with fluorescence, I tested the use of 3,3'-diaminobenzidine (DAB; see appendix III for full protocol). However, as labeling – both specific and unspecific – was similar to that seen in fluorescence tests (Appendix I, figure VII A & B), the latter was preferred.

Up to this point two different batches of primary antibody were used, ruling out the possibility of production errors. However, the third batch that was ordered did not produce results similar to those described above throughout a number of tests, as only main white matter tracts such as the corpus callosum and external capsule were stained (Appendix I, figure VII C). In parallel to the tests with the new batch, a new primary antibody (monoclonal mouse anti-connexin 36) was tested. The initial test with the new antibody only showed weak to medium signal that was specific. Yet, unspecific staining in neocortex had disappeared. The perfusion protocol was once more changed in order to obtain tissue with the best possible quality and another test with the mouse anti-connexin 36 antibody was performed (protocols for perfusion and immunohistochemistry are described in the methods section). The results for this test will be described in the following section.

3.1.2. Connexin 36

The labeling in the final experiment was evaluated to be purely specific. This was based on the fact that not only expected areas were stained exclusively, but also their staining pattern matched expectations. While fairly high levels of background staining remained, the signal-to-noise ratio was deemed sufficient for analysis.

The entire Cld was devoid of labeling (figure 7 A-C). However, labeling was seen in the Clv, yet weak and sparse compared to areas such as hippocampus (figure 8). The labeling in the Clv was mostly restricted to its more dorsomedial portion, although some labeling was also scattered in more ventral and lateral portions. Extending from around 0.36 mm to 4.44 mm behind Bregma, labeling was only seen in the posterior half of the Clv (figure 9). A gradient throughout the labeled extent was observed, by which the central portion was more densely labeled (figure 9 C & D) compared to more anterior and posterior portions (figure 9 A-B, E-F). Furthermore, both cell bodies and neurites showed the puncta staining characteristic of Cx36 labeling (Belluardo et al. 2000; Rash et al. 2000; figure 10). Most labeled cell bodies were 10µm or less in diameter with round or oval shapes. Due to the punctuate nature of the

labeling, neurites could not be characterized. As the expression of Cx36 alone does not predict the presence of functional GJs, tissue from the Cl was analyzed using EM.

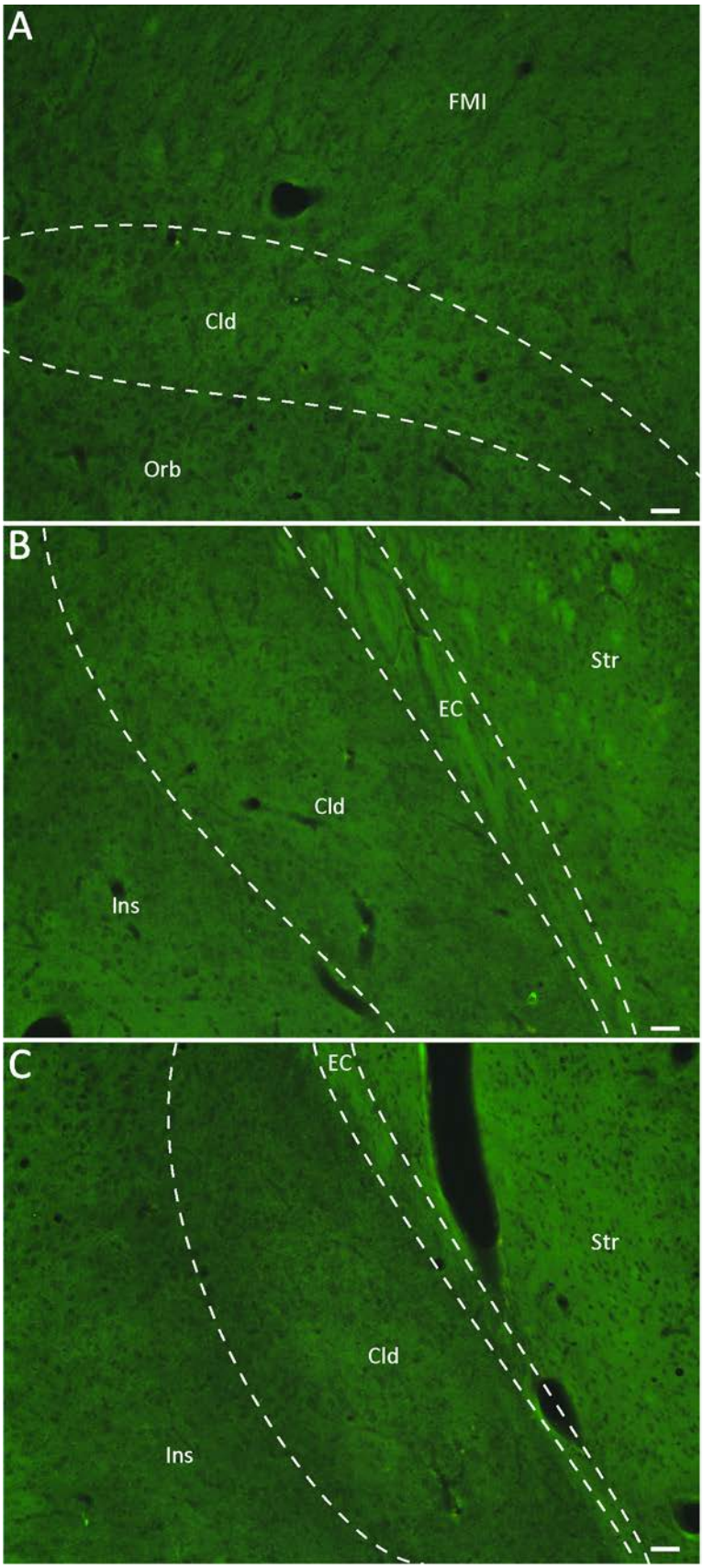

Figure 7: Absence of Cx36 staining in the dorsal claustrum using the mouse anti-Cx36 antibody. At three different antero-posterior coronal levels through the dorsal claustrum (A-C) labeling was not present.
A: 3.72mm in front of Bregma.
B: 1.92mm in front of Bregma.
C: 1.80mm behind Bregma.
Scale Bars: 50µm.
Cld - Dorsal claustrum; EC - External capsule; FMI – Forceps minor of the corpus callosum; Ins – Insular cortex; Orb – Orbitofrontal cortex; Str – Striatum.

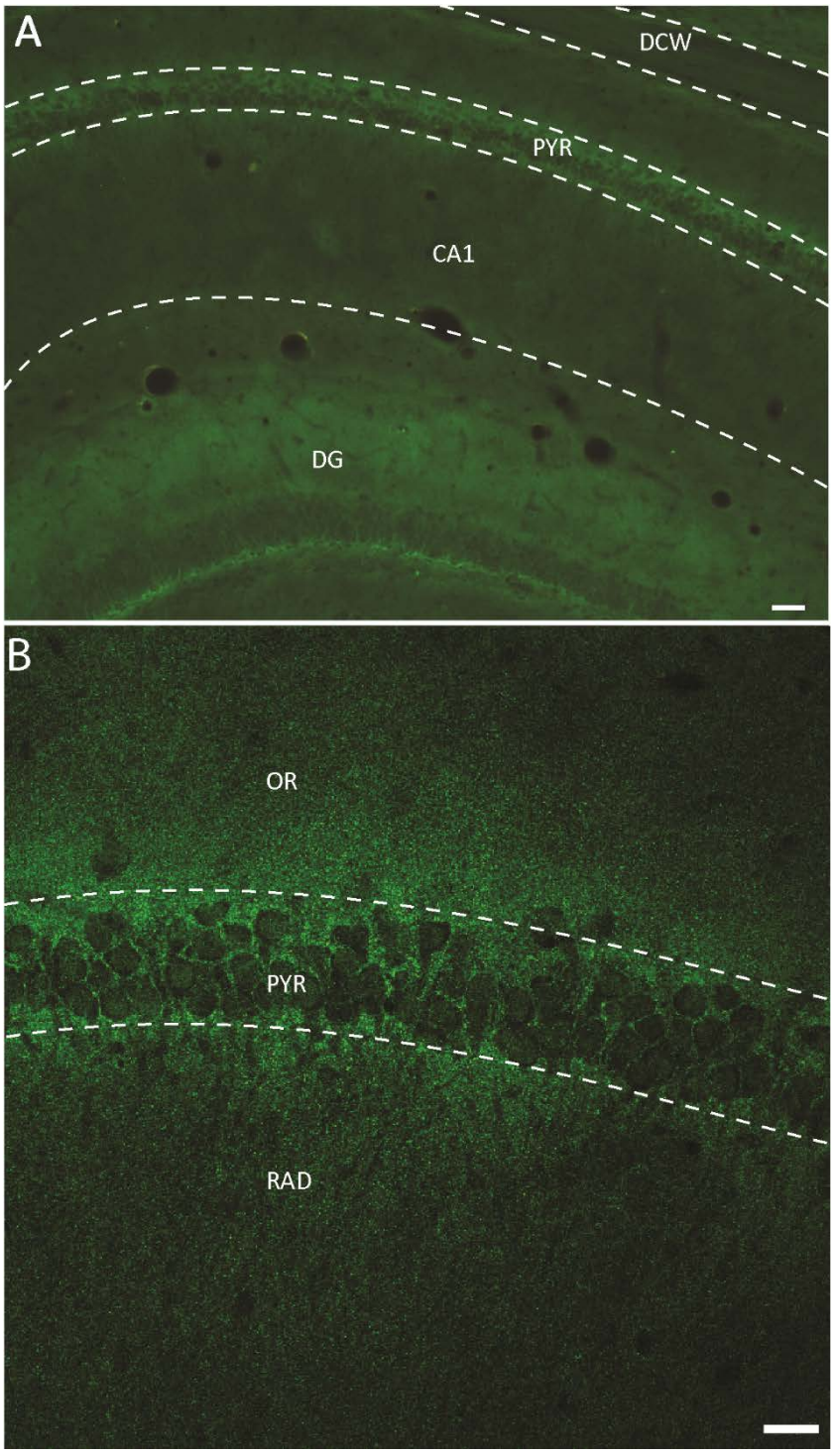

Figure 8: Comparatively strong labeling in hippocampus. A: Specific labeling in CA1 and DG. B: Confocal image of specific labeling in CA1, optical plane thickness ~8µm. Scale bar (A): 50µm. Scale bar (B): 20µm. CA1 – Cornu Ammonis 1; DCW – Deep cerebral white matter; DG – Dentate Gyrus; OR – Oriens layer of CA1; PYR – Pyramidal cell layer of CA1; RAD – Radiatum layer of CA1.

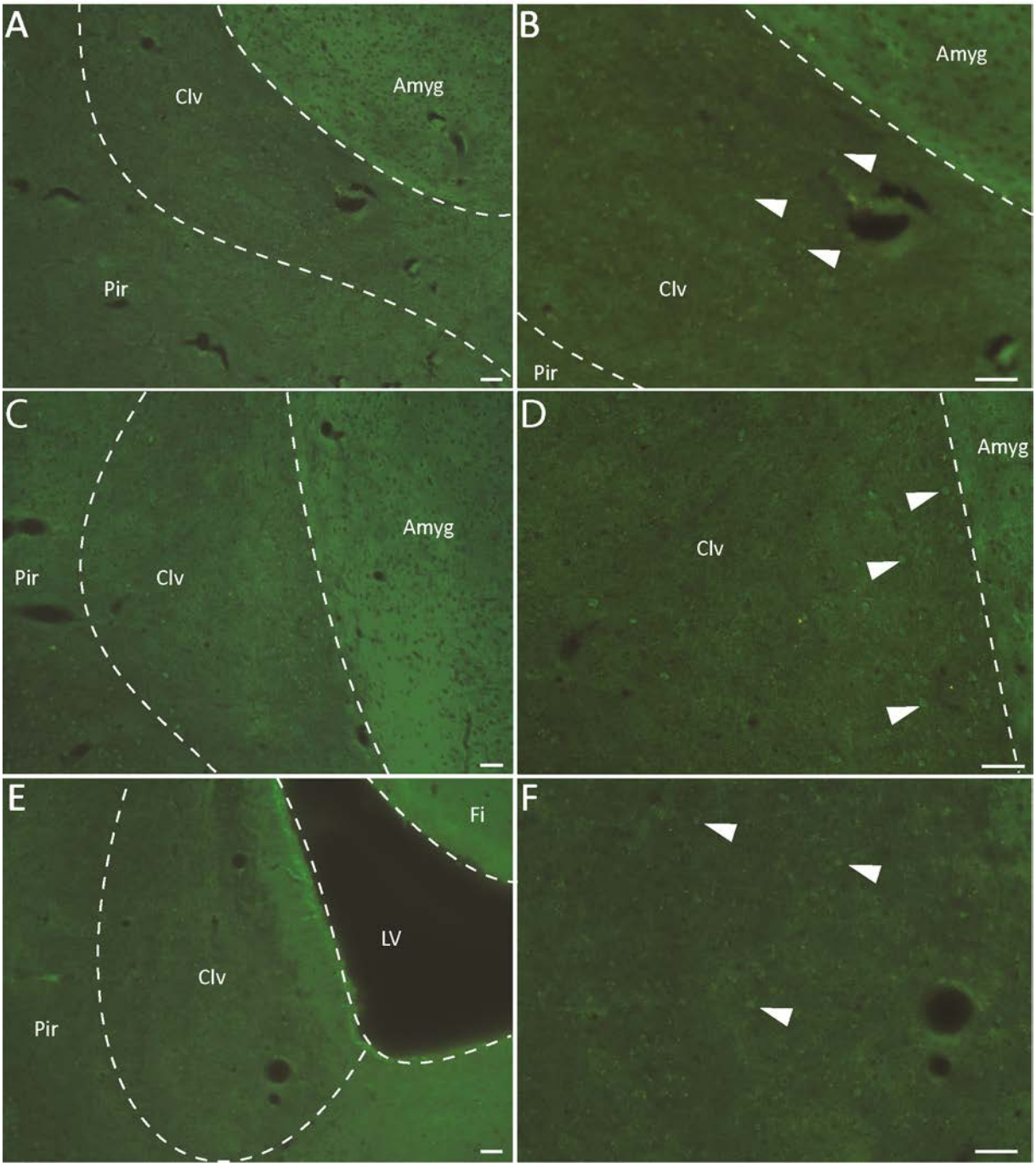

Figure 9: Cx36 staining in the posterior half of the ventral claustrum using the mouse anti-Cx36 antibody. At three different antero-posterior coronal levels through the posterior half of the ventral claustrum (A-F) labeling was present. A-B: 0.36mm behind Bregma. C-D: 2,04mm behind Bregma. E-F: 4.44mm behind Bregma. B, D, F: Arrows indicate labeled cells. Scale bars: 50µm. Amyg – Amygdala; Clv - Ventral claustrum; Fi – Fimbria of the hippocampus; LV – Lateral ventricle; Pir – Piriform cortex.

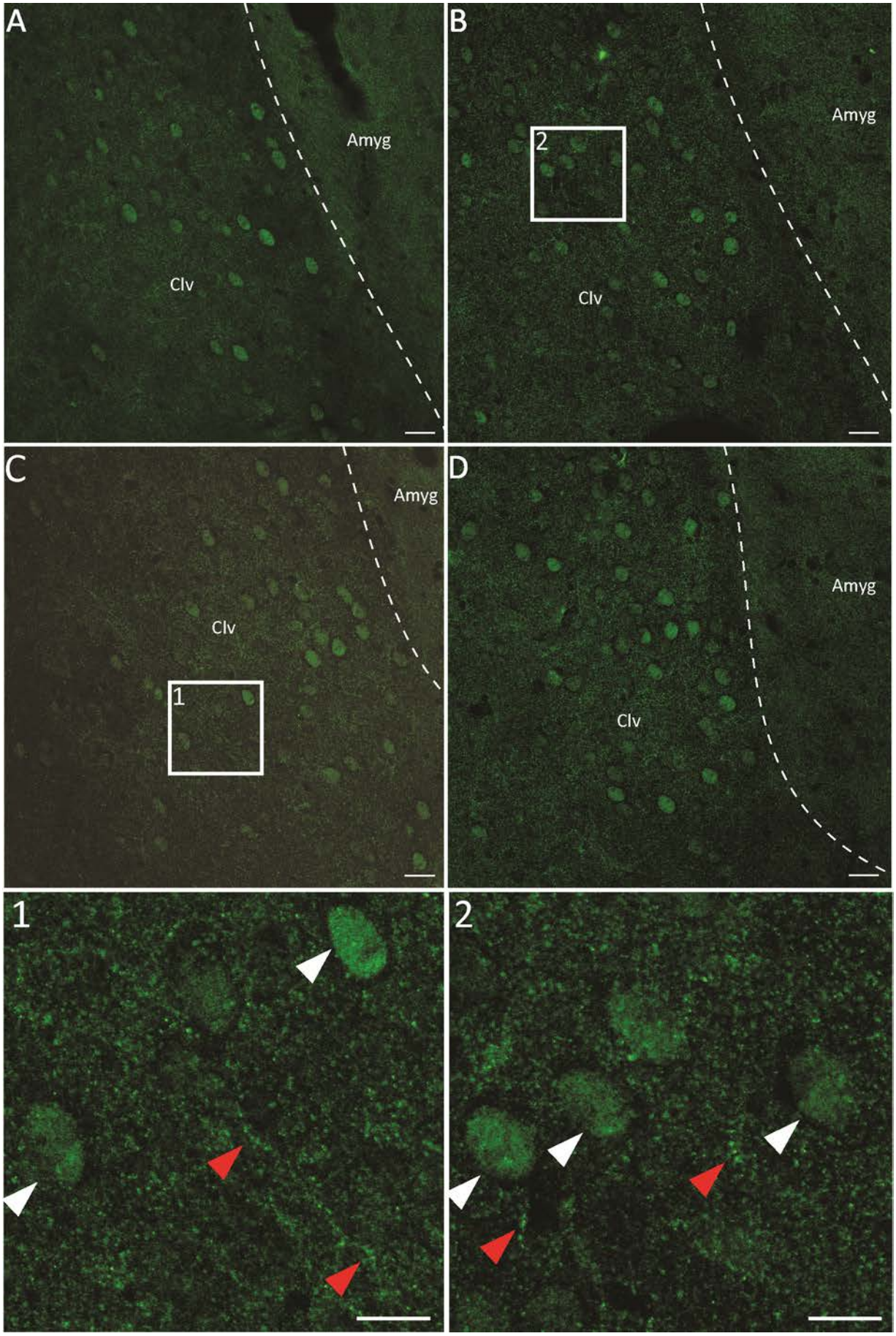
A
Amyg
Clv
B
2
Amyg
Clv
C
Amyg
Clv
1
D
Amyg
Clv
1
2

Figure 10 (Above): Confocal images of most densely labeled Clv areas, showing characteristic punctate labeling. Optical plane thickness ~7µm. White boxes indicate areas shown at higher magnification in 1 and 2. White arrows indicate cell bodies. Red arrows indicate neurites. Scale bars (A-D): 20µm. Scale bars (1, 2): 10µm. Amyg – Amygdala; Clv – Ventral claustrum.

3.2. Electron microscopy

Sections from a GAD67-eGFP positive mouse with DAB labelled eGFP (see appendix III for full protocol) were first tested. GAD67 is a commonly used interneuron marker, while interneurons themselves have been described to express Cx36 more frequently than other neurons. Thus, the main rational of this test was to aid localization of GJs with the electron microscope, while also allowing for a distinction of GJ expressing cells into GAD67 positive and negative. However, the tissue prepared for this test turned out to have poorly maintained ultrastructure – to the point that membranes were too fuzzy for analysis (figure 11). Therefore, all subsequently analyzed tissue was unlabeled.

Based on the immunolabeling in the rat described above, putative GJs were expected to be found in the Clv rather than the Cld. However, as absence of immunolabeling is no absolute indicator of GJs absence, tissue from both the Clv and Cld was analyzed. To this end, tissue from two rats (one animal per claustral portion) was investigated and split into three tissue blocks each.

Classification of GJs in electron micrographs was based on four criteria: (1) dark, dense membrane appositions; (2) periodic widenings of space between membranes; (3) a thin, electron dense band running centrally through membrane appositions; (4) visibility/continuity in consecutive sections. Furthermore, GJ-like structures close to organelles such as mitochondria or endoplasmatic reticula were disregarded, as membrane appositions often form close to organelles (figure 13 C & 24 A; Red arrows). While not all of these criteria are explicitly described elsewhere, they were derived from a number of studies showing the characteristic structure of GJs in electron micrographs (van der Want et al. 1998; Hamzei-Sichani et al. 2007; Hamzei-Sichani et al. 2012; Talaverón et al. 2014). See figure 11 for a representative example illustrating all four criteria. GJs are most commonly seen in plaque accumulations spanning a few 100nm and along several segments of the same membrane. To be able to capture these features, serial sections were analyzed.

No structures of interest (SOIs) could be observed in tissue from the Cld. Yet, seven regions with several SOIs were found in the Clv that fulfilled three of the four above described criteria – criterion three, a thin electron dense band between the two adhering membranes, being absent or ambiguous in all examples. All putative GJs were located between parallel running neurites, while none were located on cell bodies. Figures 13 and 14 show representative examples of putative GJs with both the typical close membrane appositions and recurrent widenings between membranes visible in the high-magnification micrographs. Furthermore, Figure 13 D illustrates an example of the occurrence of putative GJs on several sites between the same membrane pair. All other SOIs can be found in appendix II. It also worth noting that all putative GJs were found in close proximity of each other – i.e. the same ultrathin sections, cut from a single flat-embedded section (figure 15). Further SOIs were found in other sections of the Clv; however, they did not fulfill more than two criteria of those mentioned above and thus they were disregarded.

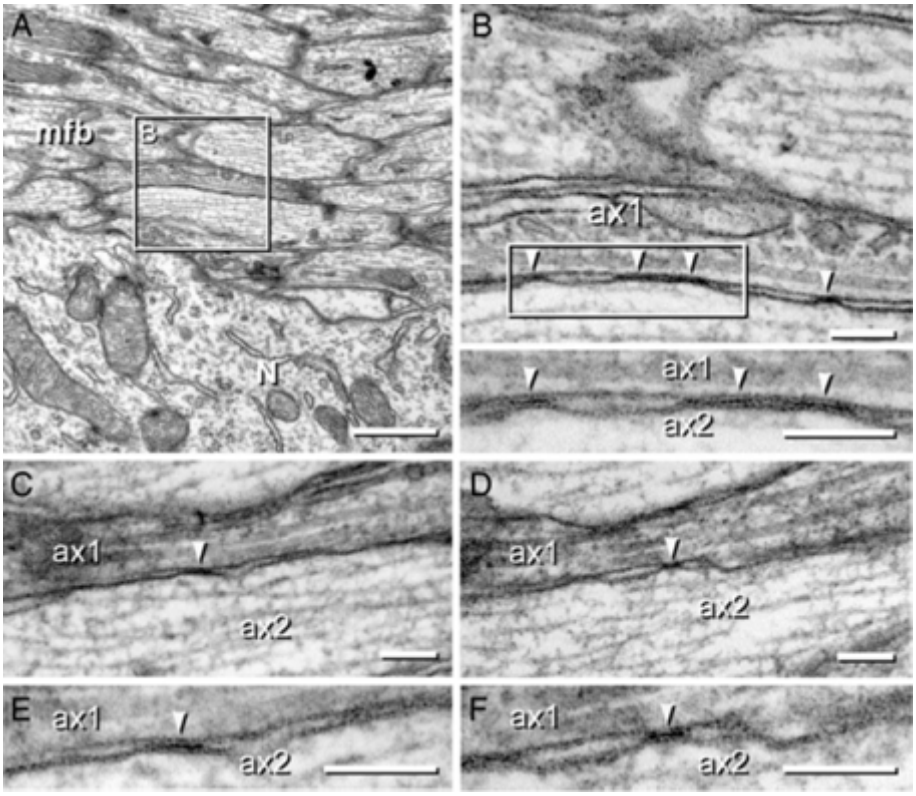

Figure 11: Electron micrograph of example GJs between two mossy fiber axons (ax1 and ax2) in adjacent sections. Showing dark, dense membrane appositions; periodic widenings between membranes; a thin, electron dense band between membrane appositions; continuity in consecutive sections. Scale bar (A): 500nm. Scale bars (B-F): 100nm. Modified from Hamzei-Sichani et al. (2007).

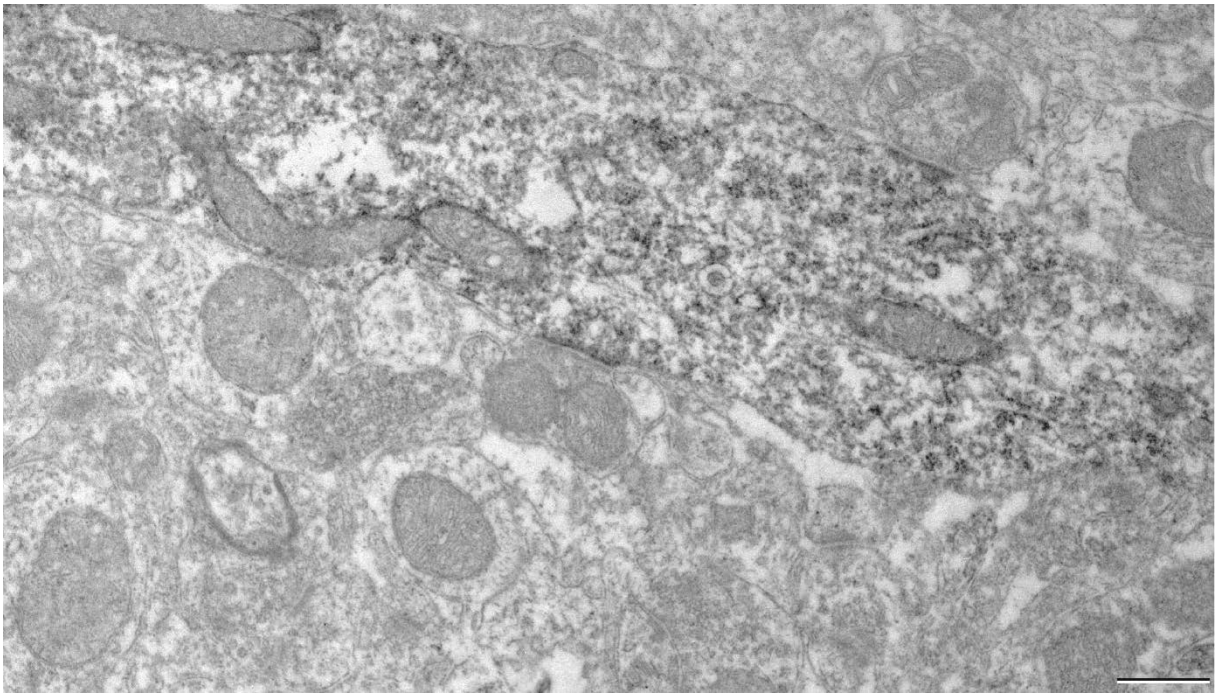

Figure 12: Test with DAB labeled eGFP, showing low quality tissue. Scale bar: 1µm

Figure 13 (bellow): Serial sections of example SOIs. Red arrow: Disregarded membrane apposition, due to proximity of mitochondrion. Black arrows indicate putative GJ. Red boxes indicate areas shown at higher magnification in 1, 2 and 3. Scale bars (A-D): 500nm. Scale bars (1-3): 50nm.

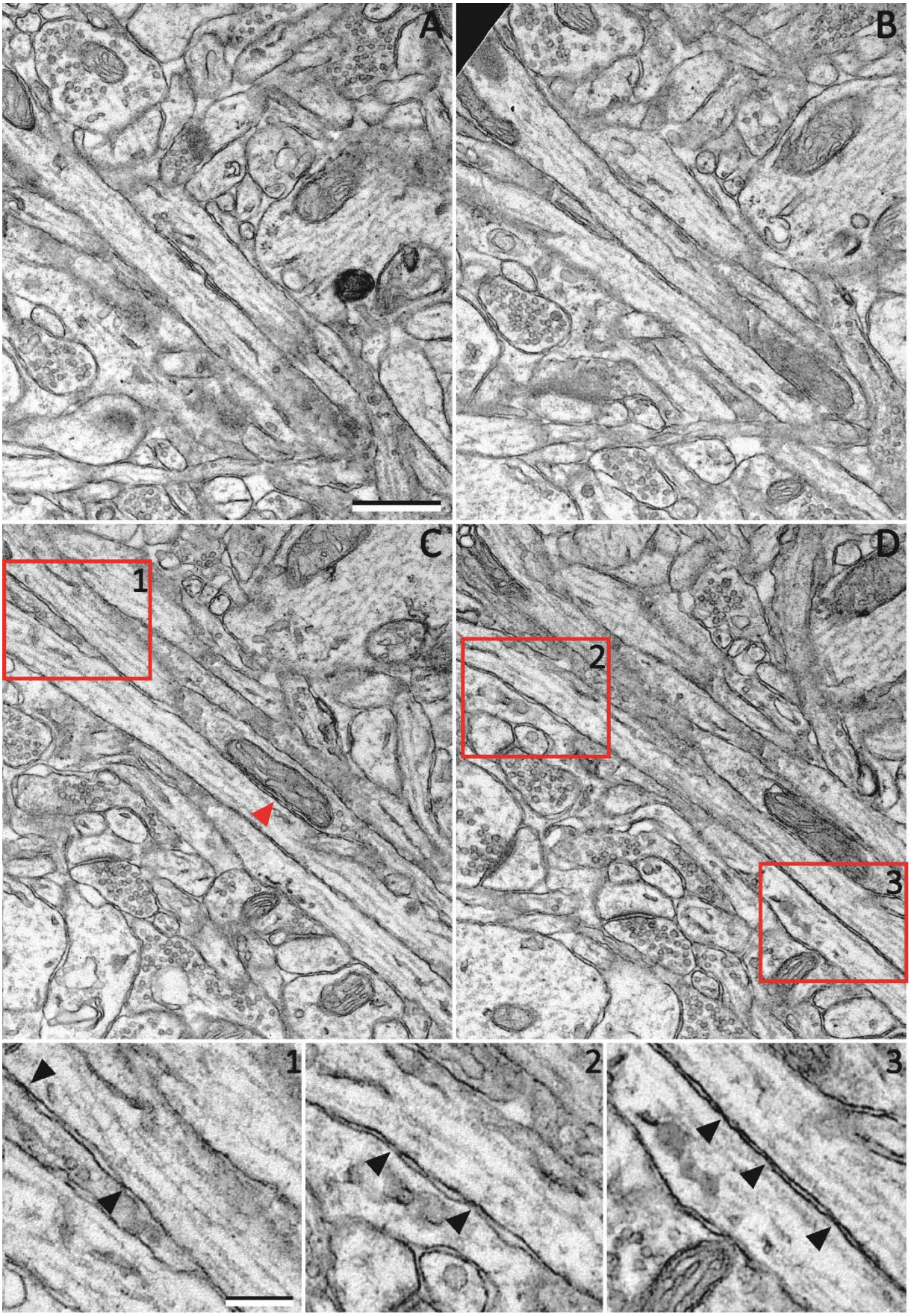
A
B
C
1
D
2
3
1
2
3

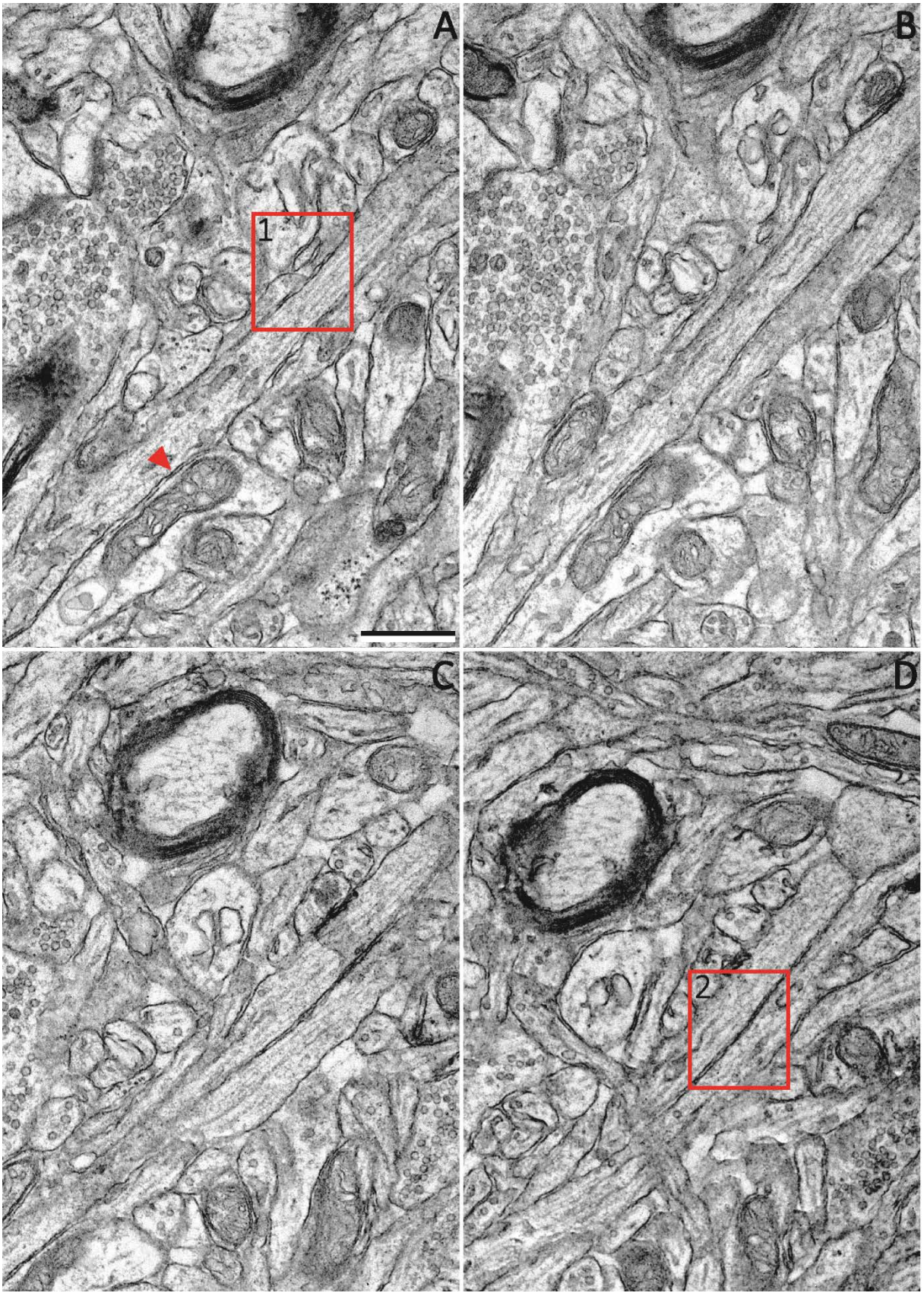

Figure 14 (continued below): Serial sections of example SOIs. Red arrow: Disregarded membrane apposition, due to proximity of mitochondrion. Black arrows indicate putative GJ. Red boxes indicate areas shown at higher magnification in 1 and 2. Scale bars (A-D): 500nm. Scale bars (1-2): 50nm.

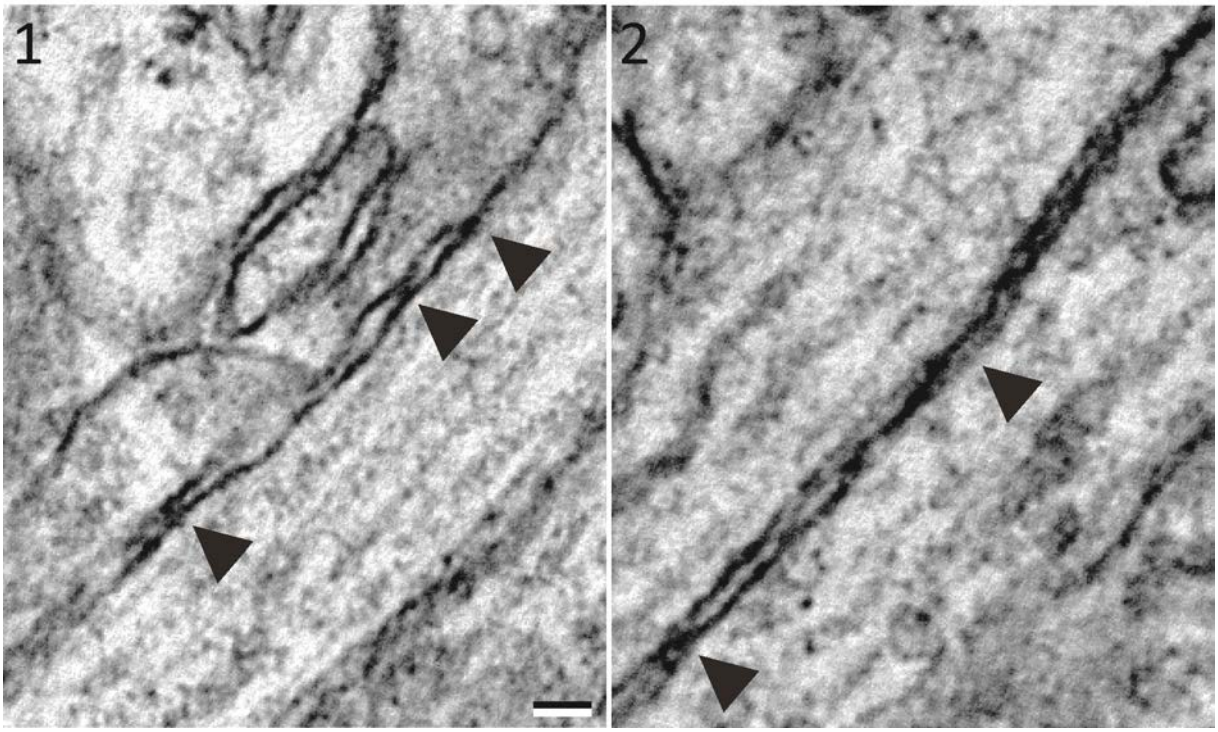

Figure 14 (Continued).

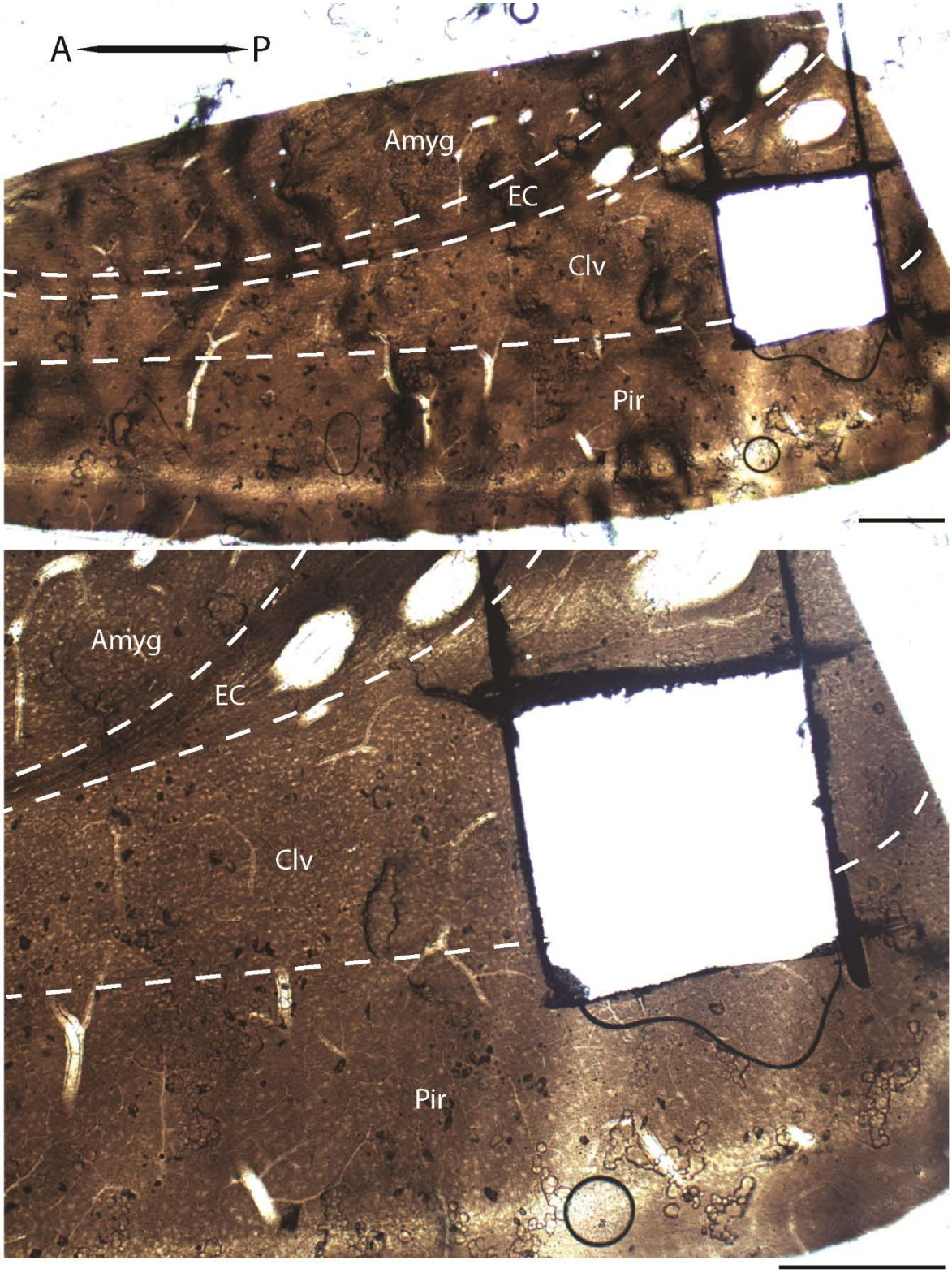

Figure 15: Flat-embedded tissue showing cut-out section of the Clv in which all SOIs were found. Scale bars: 250µm. Amyg – Amygdala; Clv – Ventral claustrum; EC – External capsule; Pir – Piriform cortex.

4. Discussion

Since the publication of Crick and Koch's (2005) hypothesis, the Cl has gained renewed interest. Nevertheless, no substantial progress has been made in elucidating the function of the Cl. Instead, further debates have been sparked, for example concerning the exact structural boundaries of the Cl (Mathur et al. 2009). Therefore, Crick and Koch's hypothesis still remains the dominant idea of what the role of the Cl may be; although, not completely uncriticized (Remedios et al. 2010; Smith et al. 2012). Many questions still surround the Cl. Under consideration of one of the most frequent assumptions in current hypotheses – the presence of GJs in the CL, the present study was conducted to investigate this suggestion.

4.1. Synopsis of main results

Initially, several issues concerning the immunohistochemical approach were encountered. Yet, these were eventually resolved by dismissal of the unreliable polyclonal rabbit anti-cx36 antibody and subsequent use of the specific monoclonal mouse anti-cx36 antibody. With the latter antibody no labeling was found throughout the Cld. However, labeling was found in the posterior half of the dorsomedial Clv. See figure 16 for a schematic representation of the labeling pattern. In agreement with this labeling pattern, no GJ-like structures were found in the Cld using EM, while several putative GJs were found in the Clv.

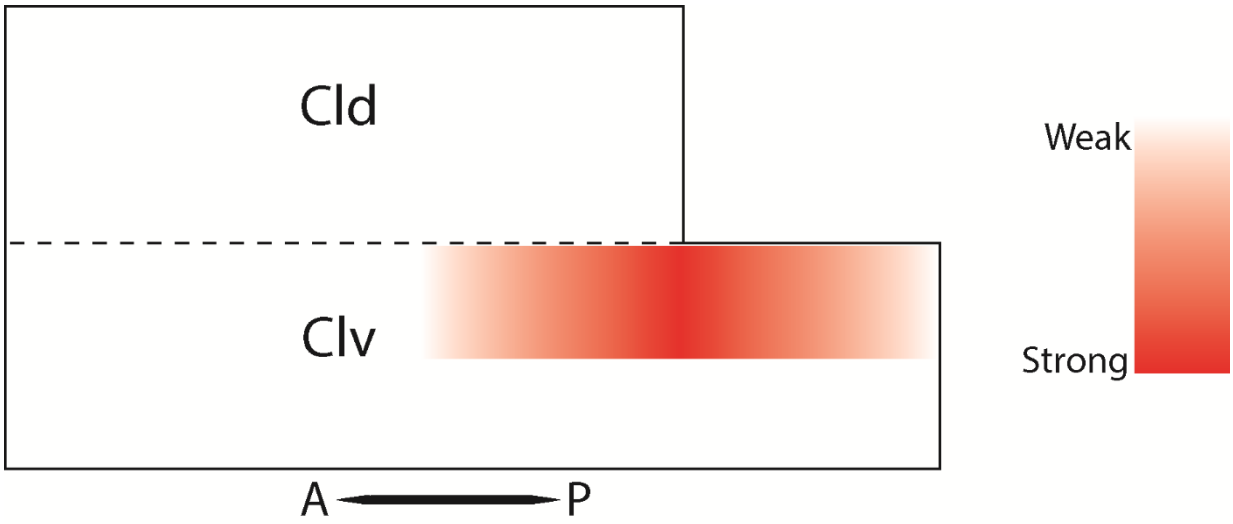

Figure 16: Schematic representation of the Cld and Clv from a sagittal perspective. The gradient of Cx36 labeling in the posterior dorsomedial Clv is represented in red.

4.2. Methodological considerations

Several issues with the methods used in the present thesis need to be considered, as they may represent confounding factors in the analysis of the results. A general problem with immunofluorescence is photo bleaching (Shaner et al. 2005). As the described signal from Cx36 positive cells and neurites was already comparatively weak in the Clv, there is a possibility that even weaker signal was lost due to photo bleaching before analysis and could thus not be identified. However, careful steps were taken to reduce photo bleaching to a minimum – such as storing sections in darkness. Thus, the described labeling most likely represents the complete picture.

A second problem specific to membrane proteins, including Cx36 is the possibility of interference from cell permeabilization agents. As these agents dissolve parts of the cell membrane, the possibility needs to be considered that some of the Cx36 was removed in this process. This would lead to a less representable labeling pattern and could explain weak labeling. To address this issue, two cell permeabilization agents of distinct strengths were tested, yielding essentially identical results. While it is therefore unlikely that there was interference from cell permeabilization agents, the possibility cannot be excluded.

A further concern is the quality of the tissue used for EM. Even a slight reduction in quality can impact the clarity of individual structures and can therefore hamper their distinction or classification. Tissue condition is tremendously dependent on the quality of perfusions. While utmost care was taken to perform top quality perfusions, pristine tissue is impossible to guarantee. Tissue quality is also reduced with increasing time between perfusion and final processing for EM. Although time between processing steps was attempted to be kept at a minimum, it remains a factor that had potential impact on the present study. Therefore, it is possible that potential GJs were overlooked, due to fuzziness of membranes resulting from potentially reduced tissue quality.

4.3. Connexin 36

Cx36 labeling was observed exclusively in the posterior half of the Clv. Within this part of the nucleus, expression was mostly restricted to its medial portion, where it was found in both cells and neurites. Localization of Cx36 is a good indicator of potential neuronal GJ presence. However, it has to be kept in mind that the labeling only represents the localization of the protein Cx36. This means that only parts of the observed signal corresponds to functional GJs, while some labeling will also represent Cx36 in other forms.

Generally Cxs have a fairly short half-life of one to five hours (Berthoud et al. 2004), with Cx36 being no exception at around 2.8 hours (Wang 2013). It has been speculated that this turnover rate is a key factor in the functional plasticity of GJs and the related regulation of inter-cell transmission of both metabolites and electric charge. As a consequence of such a quick turnover rate, large amounts of Cx36 will be constantly newly synthesized and transported to its final site of use, but also transported back for degeneration. Cxs have also been suggested to fulfill several other functions than to form GJs (for a review see Dbouk et al. 2009). As an example, Cx36-hemichannels have been described to be involved in the release of ATP from cells into extracellular space and the therewith connected tolerance to ischemia (Schock et al. 2008). Thus, some of the Cx36 labeling observed in this project may correspond to hemichannels or protein being synthesized or transported, rather than GJs.

The expression of Cx36 in the Cl has not been described previously. While whole brain analyses of Cx36 expression have been done before, these investigations mostly used *in situ* hybridization (Condorelli et al. 1998; Condorelli et al. 2000; Belluardo et al. 2000). There are several potential reasons as to why expression in the Cl was not previously reported. Firstly, the expression found in the present thesis was generally quite weak, it is therefore possible that previous studies simply dismissed it as noise. Alternatively, as the mentioned studies tended to be rather general in their descriptions of weaker signals – especially of expression in cortex – it is conceivable that the Cl was included in these definitions. Disparities between previous reports and the present one may have also resulted from the difference in

methodology. *In situ* hybridization reveals localization of mRNA, which is not always congruent with protein expression – a factor already acknowledged by some of the authors of Cx36 localization studies (Belluardo et al. 2000). Furthermore, although immunofluorescence was previously used to investigate Cx36 presence throughout the brain, differences in antibodies and their efficiencies may have produced discrepancies between results (Belluardo et al. 2000).

It is important to recognize that only the expression of Cx36 and no other Cx type was investigated. Cx36 was chosen based on its far more extensive expression throughout the brain, while other neuronal Cx types have been described in comparatively few regions (Hormuzdi et al. 2004; Söhl et al. 2005). It should still be considered that Cx45 or Cx57 may be also expressed in the Cl. Yet, based on the EM results, it is unlikely that they are expressed in any other region than the Clv.

Although it seemed possible to infer cell shape from the Cx-labeling itself, it is uncertain whether parts of the cell body remained unstained, as Cx expression may not be homogenously distributed throughout the cell. Thus, the appearance of some of the somata may have been distorted. However, if cell bodies were in fact completely labeled some inferences can be made. All labeled somata were either round or oval with most of them no bigger than 10µm. This may be the first indicator that the Cx-positive population is comprised of GABAergic neurons, as their somata shape coincides with that of GABAergic neurons in the rodent Cl (Guirado et al. 2003).

4.4. Electron Microscopy

The observations made in the EM strongly supported the results from the immunohistochemical approach. Specifically in that no GJ-like structures were found in the Cld, while several putative GJs were found in the Clv. However, although cell bodies were also expected to express GJs, putative GJs were exclusively located between parallel running neurites. Based on the results presented here, it is impossible to say whether the described putative GJs are of the Cx36 subtype or consist of another Cx type. Yet the overlap between results from the two methodological approaches used in this study strongly indicate that the putative GJs observed in the EM are composed of Cx36.

GJs were classified using four main criteria, which were based on previous reports of GJs in various types of cells using EM. In these studies, structures classified as GJs consistently showed close, electron dense membrane appositions and periodic widenings between apposed membranes (van der Want et al. 1998; Hamzei-Sichani et al. 2007; Hamzei-Sichani et al. 2012; Talaverón et al. 2014). In most cases, an electron dense band extended through the center of membrane appositions. Furthermore, one report included serial sections to show continuous expression of GJs at multiple sites of the same opposing membranes (Hamzei-Sichani et al. 2007). In most of these studies, classification as GJs of structures that had these characteristics was supported by additional methods – such as immunogold labeling or freeze facture replication – lending strong credibility to the criteria used in the present study. The structure of GJs seems to be common to all Cx types. Furthermore, the structure of GJs does not seem to change depending on the cell type or on which part of the cell they are located

on. Such universality grants ease of classification, as none of these factors have to be considered.

In the present investigation putative GJs did not show the electron dense band running between membrane appositions unambiguously. While it may be argued that this indicates misclassification of the putative GJs described here, there are two main reasons as to why this criterion may have been continuously absent. Firstly, the issue of cutting thickness of the ultrathin sections has to be factored in. Thicker sections make it increasingly difficult to see detailed aspects of structures in general – especially structures that are only a few nanometers small, such as GJs. Yet, sections cut too thin become fragile and therefore difficult to work with. Keeping cutting thickness stable at nanometer scale is incredibly challenging, thus fluctuations have to be taken into account at all times when working with EM. Therefore, the fact that no electron dense band was observed in putative GJs may be due to sections being cut too thick. The second potential reason for the absence of the electron dense band may be the angle at which tissue was sectioned. Even a slight tilt can make a structure appear to have different characteristics or simply fuzzy. Although it may not be highly likely, the possibility has to be considered that the tissue in the present study was continuously cut at angles slightly offset to the central electron dense band, making it appear fuzzy or completely disappear.

4.5. Functional Implications

Recognizing the dynamics of Cx36 GJ-networks given the distinct pattern of Cx36 distribution described here, several functional implications need to be considered. Regarding these implications in view of the limited knowledge on intrinsic connectivity of the Cl and the broad cortical network that it finds itself in, further conclusions can be made. Finally, putting the ensemble of implications into the context of the existing functional hypotheses will lead to defining a set of experiments crucial in the further investigation of the Cl.

Instrumental to how GJs shape network activity is their polarization independent bidirectional nature. This means that in a GJ-coupled cell pair hyper- or depolarization of one cell will change the membrane potential of the other cell in the same way – even at sub-threshold levels. As this process happens at a very high velocity, it enables GJ-coupled cells to align their activity with each other. Due to these properties, GJs have been implicated in facilitation of network oscillations. Here it is important to highlight the aspect of facilitation rather than creation. Cells in Cx36 knock-out mice have been shown to individually continue oscillating at similar frequencies - yet asynchronously; while the amplitude of the network oscillations was markedly reduced (Deans et al. 2001; Hormuzdi et al. 2001). In representing the temporal regulation of the joint neuronal activity in a given network, oscillations have been suggested to reflect the collective processing of a single stimulus (Singer 1999) but also the expectation of a stimulus (Engel et al. 2001). In facilitating oscillations, GJs seem to play an integral role in the shaping of stimulus representation. Yet, the more detailed dynamics of a GJ-coupled network is strongly dependent on the cell type forming the network. In the hippocampus, high-frequency oscillations (~200 Hz) have been shown to be generated by GJ-coupled principal cells (Draguhn et al. 1998). By contrast, GJ-coupled interneurons have been associated with oscillations in the gamma range (~30-70 Hz; Traub et al. 2001). Based on the observations made above, Cx36 positive neurons in the Cl are most likely GABAergic – i.e.

putative interneurons. Thus, it would be reasonable to assume that gamma oscillations may prevail in at least the part of the Cl that is coupled by GJs.

Assuming the Cx36 labeling described in the present thesis represents the exclusive localization of GJs in the Cl, only a small fragment of its cells is electronically coupled – a small sub-population of cells in the posterior half of the mediodorsal Clv. Studies on the rat indicate that the Clv receives input from the infralimbic, piriform and insular cortex (Shi & Cassell 1998a; Shi & Cassell 1998b; Schwabe et al. 2004; Vertes 2004), while it projects to the piriform, perirhinal, entorhinal, agranular insular, orbital, prelimbic and infralimbic cortex (Behan & Haberly 1999; Hoover & Vertes 2007). With the exception of the piriform and insular cortex, all cortical areas connecting to the Clv are at high levels in the cortical hierarchy. While the exception of piriform and insular cortex could be explained by their proximity to the Clv, the reason for a preferential connectivity with higher order cortices is more challenging to resolve. Given the role of GJs in synchronized activity, the question also arises as to why the inputs and outputs of this specific claustral area need to be synchronized, while that of other parts of the Cl do not. However, based on the existing literature the exact efferent and afferent projections of the Cx36-positive cell population remain difficult to determine, as descriptions are usually kept general to the Clv. The possibility also has to be considered that parts of the brain are specifically connected to the Cx36-positive sub-population. Before the exact connectivity of the Cx36-positive cell population is known, it remains challenging to draw conclusions on the specific functions of this electronically coupled network.

With regard to Crick and Koch's (2005) hypothesis, the present study raises a few questions. The hypothesis postulates a widespread network within the Cl, capable of synchronizing incoming information. Several types of connections are proposed to meet this postulate, yet GJs are specifically mentioned as the most likely synchronizing mechanism. Based on the present study, it is questionable whether the small GJ-network observed here would be sufficient to fulfill the task suggested by Crick and Koch. Firstly, the limited extent of the GJ-network puts tight restrictions on the computational power of the network, casting doubt on its ability to synchronize the entire input to the Cl. Secondly, for the GJ-network to have access to all information arriving in the Cl, a second intrinsic and more extensive network would have to be in place. There are indications for such a network, based on suggested projections (Behan & Haberly 1999) and descriptions of potentially locally projecting cells (Brand 1981). How extensive this intrinsic network is and what type of connections it forms is yet to be seen. Nevertheless, assuming there is a more extensive intrinsic network, this would add at least one synaptic step between cortical areas and the GJ-network in the Cl. Such an addition would slow down the transmission of information to the GJ-network substantially, thus failing the point of rapid synchronization within the Cl. Finally, it is seems unlikely that such a small network would be in charge of synchronizing the entire brain. This is underscored by the implications this would have in an evolutionary context. Damage to the GJ-network would have much too far reaching consequences for it to be evolutionary viable. Under consideration of the above mentioned arguments, it is rather unlikely that the GJ-network described here fulfills the function proposed by Crick and Koch.

4.6. Future Directions

The methods used in the present study are not entirely capable of providing a definite answer as to whether there are GJs in the Cl, but certainly indicate their presence. Therefore, it is necessary to fully confirm the localization of GJs. To do this the most effective approach would be the use of concurrent recordings from cells in the Cl. The permeable nature of GJs to ionic current permits their detection by measuring the membrane and transjunctional potentials of two or more cells under current- or voltage clamp. This method also has the benefit that cells can be additionally injected with a fluorescent dye – e.g. biocytin – that spreads through GJs, thereby labeling coupled cells along with the injected cell. While dye injections can be used to support the results from recordings, they also enable the description of cell morphology.

In the case of confirmed presence of GJs in the Cl, several aspects will be important to investigate. First of all, the type(s) of electronically coupled cells needs to be described – specifically whether they are excitatory or inhibitory. This factor is of major concern, as it will define the general dynamics of the GJ-coupled network, as explained above. Again, this could best be done using an electrophysiological approach. Secondly, the exact connectivity of the GJ-coupled cell population should be determined, both with the rest of the Cl and other areas of the brain. Viral tracing techniques would be most appropriate to approach this problem, as they make it possible to target specific cell populations. Exploring the connectivity of the GJ-network in the Cl would yield major insights into what the possible function of this specific cell population may be.

Lastly, it would also be of interest to compare the occurrence of GJs across species. As described in several sections of this thesis, aspects such as general morphology, connectivity and the expression of molecular markers can vary substantially across species. Thus, it would not be surprising if – in animals other than rats – GJs were either not at all present or expressed in a different area of the Cl than described in the present study. Differences and similarities between species may give further insights into what the specific function of the GJ-coupled network could be.

4.7. Conclusion

In the past, the Cl has proven to be remarkably challenging to investigate and continues to be so. The present study investigated one of many unresolved issues pertaining to the Cl – its intrinsic connectivity. Subject to this study was the potential presence of GJs, chosen for their role in synchronizing neural networks. While GJs had previously been postulated to be expressed in the Cl, there has been no support for this claim to date. Here first indications are presented of the localization and some of the likely characteristics of GJs in the Cl. Both immunohistochemical and EM approaches showed no putative GJs in the Cld. By contrast, a small population of Cx36 positive cells were found in the posterior half of the mediodorsal Clv. EM results support the notion that this portion of the Clv expresses GJs. Together these results cast doubt on current functional hypotheses that rely on a wide GJ-network throughout the Cl. The definitive function of the claustrum remains enigmatic and promises to remain so for now.

5. References

Arimatsu, Y., Kojima, M. & Ishida, M., 1999. Area- and lamina-specific organization of a neuronal subpopulation defined by expression of latexin in the rat cerebral cortex. *Neuroscience*, 88(1), pp.93–105.

Arimatsu, Y., Nihonmatsu, I. & Hatanaka, Y., 2009. Localization of latexin-immunoreactive neurons in the adult cat cerebral cortex and claustrum/endopiriform formation. *Neuroscience*, 162(4), pp.1398–410.

Ashwell, K.W.S., Hardman, C. & Paxinos, G., 2004. The claustrum is not missing from all monotreme brains. *Brain, behavior and evolution*, 64(4), pp.223–41.

Baizer, J.S., 2001. Serotonergic innervation of the primate claustrum. *Brain research bulletin*, 55(3), pp.431–4.

Bayer, S.A. & Altman, J., 1991. Development of the endopiriform nucleus and the claustrum in the rat brain. *Neuroscience*, 45(2), pp.391–412.

Behan, M. & Haberly, L.B., 1999. Intrinsic and efferent connections of the endopiriform nucleus in rat. *The Journal of comparative neurology*, 408(4), pp.532–48.

Belluardo, N. et al., 2000. Expression of connexin36 in the adult and developing rat brain. *Brain research*, 865(1), pp.121–38.

Beneyto, M. & Prieto, J.J., 2001. Connections of the auditory cortex with the claustrum and the endopiriform nucleus in the cat. *Brain research bulletin*, 54(5), pp.485–98.

Berthoud, V.M. et al., 2004. Pathways for degradation of connexins and gap junctions. *Cardiovascular research*, 62(2), pp.256–67.

Braak, H. & Braak, E., 1982. Neuronal types in the claustrum of man. *Anatomy and embryology*, 163(4), pp.447–60.

Brand, S., 1981. A serial section Golgi analysis of the primate claustrum. *Anatomy and embryology*, 162(4), pp.475–88.

Brodmann, K., 1909. *Vergleichende Lokalisationslehre der Grosshirnrinde in ihren Prinzipien dargestellt aufgrund des Zellenbaues*, Leipzig: Johann Ambrosius Barth.

Buchanan, K.J. & Johnson, J.I., 2011. Diversity of spatial relationships of the claustrum and insula in branches of the mammalian radiation. *Annals of the New York Academy of Sciences*, 1225 Suppl, pp.E30–63.

Bukauskas, F.F. et al., 2002. Coupling asymmetry of heterotypic connexin 45/ connexin 43-EGFP gap junctions: properties of fast and slow gating mechanisms. *Proceedings of the National Academy of Sciences of the United States of America*, 99(10), pp.7113–8.

Butler, A.B., Molnár, Z. & Manger, P.R., 2002. Apparent absence of claustrum in monotremes: implications for forebrain evolution in amniotes. *Brain, behavior and evolution*, 60(4), pp.230–40.

Celio, M.R., 1990. Calbindin D-28k and parvalbumin in the rat nervous system. *Neuroscience*, 35(2), pp.375–475.

Clarey, J.C. & Irvine, D.R., 1986. Auditory response properties of neurons in the claustrum and putamen of the cat. *Experimental brain research.*, 61(2), pp.432–7.

Colechio, E.M. & Alloway, K.D., 2009. Differential topography of the bilateral cortical projections to the whisker and forepaw regions in rat motor cortex. *Brain structure & function*, 213(4-5), pp.423–39.

Condorelli, D.F. et al., 1998. Cloning of a new gap junction gene (Cx36) highly expressed in mammalian brain neurons. *The European journal of neuroscience*, 10(3), pp.1202–8.

Condorelli, D.F. et al., 2000. Expression of Cx36 in mammalian neurons. *Brain research. Brain research reviews*, 32(1), pp.72–85.

Connors, B.W. & Long, M.A., 2004. Electrical synapses in the mammalian brain. *Annual review of neuroscience*, 27, pp.393–418.

Crick, F.C. & Koch, C., 2005. What is the function of the claustrum? *Philosophical transactions of the Royal Society of London. Series B, Biological sciences*, 360(1458), pp.1271–9.

Dávila, J.C. et al., 2005. Embryonic and postnatal development of GABA, calbindin, calretinin, and parvalbumin in the mouse claustral complex. *The Journal of comparative neurology*, 481(1), pp.42–57.

Dbouk, H. a et al., 2009. Connexins: a myriad of functions extending beyond assembly of gap junction channels. *Cell communication and signaling : CCS*, 7(4).

Deans, M.R. et al., 2001. Synchronous activity of inhibitory networks in neocortex requires electrical synapses containing connexin36. *Neuron*, 31(3), pp.477–85.

Draguhn, A. et al., 1998. Electrical coupling underlies high-frequency oscillations in the hippocampus in vitro. *Nature*, 394(6689), pp.189–92.

Druga, R., 1966. The claustrum of the cat (Felis domestica). *Folia morphologica*, 14(1), pp.7–16.

Edelstein, L.R. & Denaro, F.J., 2004. The claustrum: a historical review of its anatomy, physiology, cytochemistry and functional significance. *Cellular and molecular biology (Noisy-le-Grand, France)*, 50(6), pp.675–702.

Edelstein L.R. et al., 2010. Parvalbumin and neuropeptide Y immunoreactivity in the human claustrum. S*ociety for Neuroscience, 40th Annual Meeting*, Abstract #900.1.

Engel, A.K., Fries, P. & Singer, W., 2001. Dynamic predictions: oscillations and synchrony in top-down processing. *Nature reviews. Neuroscience*, 2(10), pp.704–16.

Erickson, S.L., Melchitzky, D.S. & Lewis, D.A., 2004. Subcortical afferents to the lateral mediodorsal thalamus in cynomolgus monkeys. *Neuroscience*, 129(3), pp.675–90.

Ettlinger, G. & Wilson, W.A., 1990. Cross-modal performance: behavioural processes, phylogenetic considerations and neural mechanisms. *Behavioural brain research*, 40(3), pp.169–92.

Fukuda, T. et al., 2006. Gap junctions among dendrites of cortical GABAergic neurons establish a dense and widespread intercolumnar network. *The Journal of neuroscience : the official journal of the Society for Neuroscience*, 26(13), pp.3434–43.

González-Nieto, D. et al., 2008. Regulation of neuronal connexin-36 channels by pH. *Proceedings of the National Academy of Sciences of the United States of America*, 105(44), pp.17169–74.

Goyal, V.K., 1982. Lipofuscin pigment accumulation in human brain during aging. *Experimental gerontology*, 17(6), pp.481–7.

Guirado, S. et al., 2003. Distinct types of nitric oxide-producing neurons in the developing and adult mouse claustrum. *The Journal of comparative neurology*, 465(3), pp.431–44.

Hadjikhani, N. & Roland, P.E., 1998. Cross-modal transfer of information between the tactile and the visual representations in the human brain: A positron emission tomographic study. *The Journal of neuroscience : the official journal of the Society for Neuroscience*, 18(3), pp.1072–84.

Hamzei-Sichani, F. et al., 2007. Gap junctions on hippocampal mossy fiber axons demonstrated by thin-section electron microscopy and freeze fracture replica immunogold labeling. *Proceedings of the National Academy of Sciences of the United States of America*, 104(30), pp.12548–53.

Hamzei-Sichani, F. et al., 2012. Mixed Electrical-Chemical Synapses in Adult Rat Hippocampus are Primarily Glutamatergic and Coupled by Connexin-36. *Frontiers in neuroanatomy*, 6, p.13.

Hinova-Palova, D. V et al., 2007. Parvalbumin in the cat claustrum: ultrastructure, distribution and functional implications. *Acta histochemica*, 109(1), pp.61–77.

Hinova-Palova, D. V et al., 2013. Parvalbumin-immunoreactive neurons in the human claustrum. *Brain structure & function*. Electronic publication ahead of print.

Hoffman, W.H. & Haberly, L.B., 1993. Role of synaptic excitation in the generation of bursting-induced epileptiform potentials in the endopiriform nucleus and piriform cortex. *Journal of neurophysiology*, 70(6), pp.2550–61.

Hoover, W.B. & Vertes, R.P., 2007. Anatomical analysis of afferent projections to the medial prefrontal cortex in the rat. *Brain structure & function*, 212(2), pp.149–79.

Hormuzdi, S.G. et al., 2004. Electrical synapses: a dynamic signaling system that shapes the activity of neuronal networks. *Biochimica et biophysica acta*, 1662(1-2), pp.113–37.

Hormuzdi, S.G. et al., 2001. Impaired electrical signaling disrupts gamma frequency oscillations in connexin 36-deficient mice. *Neuron*, 31(3), pp.487–95.

Hur, E.E. & Zaborszky, L., 2005. Vglut2 afferents to the medial prefrontal and primary somatosensory cortices: a combined retrograde tracing in situ hybridization study [corrected]. *The Journal of comparative neurology*, 483(3), pp.351–73.

Irvine, D.R. & Brugge, J.F., 1980. Afferent and efferent connections between the claustrum and parietal association cortex in cat: a horseradish peroxidase and autoradiographic study. *Neuroscience letters*, 20(1), pp.5–10.

Jakubowska-Sadowska, K. et al., 1998. Visual zone of the claustrum shows localizational and organizational differences among rat, guinea pig, rabbit and cat. *Anatomy and embryology*, 198(1), pp.63–72.

Katz, L.C., 1987. Local circuitry of identified projection neurons in cat visual cortex brain slices. *The Journal of neuroscience : the official journal of the Society for Neuroscience*, 7(4), pp.1223–49.

Kaufman, E.F. & Rosenquist, A.C., 1985. Efferent projections of the thalamic intralaminar nuclei in the cat. *Brain research*, 335(2), pp.257–79.

Kowiański, P. et al., 2009. Colocalization of neuropeptides with calcium-binding proteins in the claustral interneurons during postnatal development of the rat. *Brain research bulletin*, 80(3), pp.100–6.

Kowiański, P. et al., 1999. Comparative anatomy of the claustrum in selected species: A morphometric analysis. *Brain, behavior and evolution*, 53(1), pp.44–54.

Kowiański, P. et al., 2008. NPY-, SOM- and VIP-containing interneurons in postnatal development of the rat claustrum. *Brain research bulletin*, 76(6), pp.565–71.

Kowiański, P., Timmermans, J.P. & Moryś, J., 2001. Differentiation in the immunocytochemical features of intrinsic and cortically projecting neurons in the rat claustrum -- combined immunocytochemical and axonal transport study. *Brain research*, 905(1-2), pp.63–71.

Kuchiiwa, S. et al., 1984. Afferents to the cortical pupillo-constrictor areas of the cat, traced with HRP. *Experimental brain research*, 54(2), pp.377–81.

Kuchiiwa, S. et al., 1985. Efferent connections of area 20 in the cat: HRP-WGA and autoradiographic studies. *Experimental brain research*, 60(1), pp.179–83.

Künzle, H., 1975. Bilateral projections from precentral motor cortex to the putamen and other parts of the basal ganglia. An autoradiographic study in Macaca fascicularis. *Brain research*, 88(2), pp.195–209.

Künzle, H., 1977. Projections from the primary somatosensory cortex to basal ganglia and thalamus in the monkey. *Experimental brain research*, 30(4), pp.481–92.

Leichnetz, G.R., 2001. Connections of the medial posterior parietal cortex (area 7m) in the monkey. *The Anatomical record*, 263(2), pp.215–36.

LeVay, S., 1986. Synaptic organization of claustral and geniculate afferents to the visual cortex of the cat. *The Journal of neuroscience : the official journal of the Society for Neuroscience*, 6(12), pp.3564–75.

LeVay, S. & Sherk, H., 1981. The visual claustrum of the cat. I. Structure and connections. *The Journal of neuroscience : the official journal of the Society for Neuroscience*, 1(9), pp.956–80.

Lysakowski, A., Standage, G.P. & Benevento, L.A., 1988. An investigation of collateral projections of the dorsal lateral geniculate nucleus and other subcortical structures to cortical areas V1 and V4 in the macaque monkey: a double label retrograde tracer study. *Experimental brain research*, 69(3), pp.651–61.

Majak, K. et al., 2002. Projections from the amygdaloid complex to the claustrum and the endopiriform nucleus: a Phaseolus vulgaris leucoagglutinin study in the rat. *The Journal of comparative neurology*, 451(3), pp.236–49.

Majak, K. et al., 2000. The limbic zone of the rabbit and rat claustrum: a study of the claustrocingulate connections based on the retrograde axonal transport of fluorescent tracers. *Anatomy and embryology*, 201(1), pp.15–25.

Mamos, L., Narkiewicz, O. & Moryś, J., 1986. Neurons of the claustrum in the cat; a Golgi study. *Acta neurobiologiae experimentalis*, 46(4), pp.171–8.

Mathur, B.N., Caprioli, R.M. & Deutch, A.Y., 2009. Proteomic analysis illuminates a novel structural definition of the claustrum and insula. *Cerebral cortex (New York, N.Y. : 1991)*, 19(10), pp.2372–9.

Maxeiner, S. et al., 2003. Spatiotemporal transcription of connexin45 during brain development results in neuronal expression in adult mice. *Neuroscience*, 119(3), pp.689–700.

McKenna, J.T. & Vertes, R.P., 2004. Afferent projections to nucleus reuniens of the thalamus. *The Journal of comparative neurology*, 480(2), pp.115–42.

Meynert, T., 1884. *Psychiatrie. Klinik der Erkrankungen des Vorderhirns begründet aud dessen Bau, Leistungen und Ernährung.*, Vienna: Wilhelm Braumüller Universitäts-Verlagsbuchhandlung.

Minciacchi, D. et al., 1985. The organization of the ipsi- and contralateral claustrocortical system in rat with notes on the bilateral claustrocortical projections in cat. *Neuroscience*, 16(3), pp.557–76.

Minciacchi, D., Granato, A. & Barbaresi, P., 1991. Organization of claustro-cortical projections to the primary somatosensory area of primates. *Brain research*, 553(2), pp.309–12.

Miyashita, T. et al., 2005. Strong expression of NETRIN-G2 in the monkey claustrum. *Neuroscience*, 136(2), pp.487–96.

Neal, J.W., Pearson, R.C. & Powell, T.P., 1986. The relationship between the auditory cortex and the claustrum in the cat. *Brain research*, 366(1-2), pp.145–51.

Olson, C.R. & Graybiel, A.M., 1980. Sensory maps in the claustrum of the cat. *Nature*, 288(5790), pp.479–81.

Paxinos, G. & Watson, C., 2007. *The Rat Brain in Stereotaxic Coordinates* 6th ed., Academic Press.

Pearson, R.C. et al., 1982. The organization of the connections between the cortex and the claustrum in the monkey. *Brain research*, 234(2), pp.435–41.

Pirone, A. et al., 2012. Topography of Gng2- and NetrinG2-expression suggests an insular origin of the human claustrum. *PloS one*, 7(9), p.e44745.

Puelles, L. et al., 2000. Pallial and subpallial derivatives in the embryonic chick and mouse telencephalon, traced by the expression of the genes Dlx-2, Emx-1, Nkx-2.1, Pax-6, and Tbr-1. *The Journal of comparative neurology*, 424(3), pp.409–38.

Rahman, F.E. & Baizer, J.S., 2007. Neurochemically defined cell types in the claustrum of the cat. *Brain research*, 1159, pp.94–111.

Rash, J.E. et al., 2000. Immunogold evidence that neuronal gap junctions in adult rat brain and spinal cord contain connexin-36 but not connexin-32 or connexin-43. *Proceedings of the National Academy of Sciences of the United States of America*, 97(13), pp.7573–8.

Real, M.A., Dávila, J.C. & Guirado, S., 2003. Expression of calcium-binding proteins in the mouse claustrum. *Journal of chemical neuroanatomy*, 25(3), pp.151–60.

Real, M.A., Dávila, J.C. & Guirado, S., 2006. Immunohistochemical localization of the vesicular glutamate transporter VGLUT2 in the developing and adult mouse claustrum. *Journal of chemical neuroanatomy*, 31(3), pp.169–77.

Reblet, C. et al., 2002. Neuroepithelial origin of the insular and endopiriform parts of the claustrum. *Brain research bulletin*, 57(3-4), pp.495–7.

Remedios, R., Logothetis, N.K. & Kayser, C., 2010. Unimodal responses prevail within the multisensory claustrum. *The Journal of neuroscience : the official journal of the Society for Neuroscience*, 30(39), pp.12902–7.

Reynhout, K. & Baizer, J.S., 1999. Immunoreactivity for calcium-binding proteins in the claustrum of the monkey. *Anatomy and embryology*, 199(1), pp.75–83.

Roberts, A. & Tomic, D., 2007. Forebrain connectivity of the prefrontal cortex in the marmoset monkey (Callithrix jacchus): An anterograde and retrograde tract-tracing study. *Journal of Comparative Neurology*, 502(1), pp.86–112.

Sadowski, M. et al., 1997. Rat's claustrum shows two main cortico-related zones. *Brain research*, 756(1-2), pp.147–52.

Schmitz, D. et al., 2001. Axo-axonal coupling. a novel mechanism for ultrafast neuronal communication. *Neuron*, 31(5), pp.831–40.

Schock, S.C. et al., 2008. ATP release by way of connexin 36 hemichannels mediates ischemic tolerance in vitro. *Biochemical and biophysical research communications*, 368(1), pp.138–44.

Schwabe, K., Ebert, U. & Löscher, W., 2004. The central piriform cortex: anatomical connections and anticonvulsant effect of GABA elevation in the kindling model. *Neuroscience*, 126(3), pp.727–41.

Segundo, J.P. & Machene, X., 1956. Unitary responses to afferent volleys in lenticular nucleus and claustrum. *Journal of neurophysiology*, 19(4), pp.325–39.

Shaner, N.C., Steinbach, P.A. & Tsien, R.Y., 2005. A guide to choosing fluorescent proteins. *Nature methods*, 2(12), pp.905–9.

Sherk, H. & LeVay, S., 1983. Contribution of the cortico-claustral loop to receptive field properties in area 17 of the cat. *The Journal of neuroscience : the official journal of the Society for Neuroscience*, 3(11), pp.2121–7.

Shi, C.J. & Cassell, M.D., 1998a. Cascade projections from somatosensory cortex to the rat basolateral amygdala via the parietal insular cortex. *The Journal of comparative neurology*, 399(4), pp.469–91.

Shi, C.J. & Cassell, M.D., 1998b. Cortical, thalamic, and amygdaloid connections of the anterior and posterior insular cortices. *The Journal of comparative neurology*, 399(4), pp.440–68.

Shi, S.-R., Shi, Y. & Taylor, C.R., 2011. Antigen retrieval immunohistochemistry: review and future prospects in research and diagnosis over two decades. *The journal of histochemistry and cytochemistry : official journal of the Histochemistry Society*, 59(1), pp.13–32.

Shibuya, H. & Yamamoto, T., 1998. Electrophysiological and morphological features of rat claustral neurons: an intracellular staining study. *Neuroscience*, 85(4), pp.1037–49.

Singer, W., 1999. Neuronal synchrony: a versatile code for the definition of relations? *Neuron*, 24(1), pp.49–65, 111–25.

Słoniewski, P., 1983. Pretectal connections to the claustrum: an HRP retrograde transport study in cats. *Acta neurobiologiae experimentalis*, 43(3), pp.165–82.

Sloniewski, P., Usunoff, K.G. & Pilgrim, C., 1986. Diencephalic and mesencephalic afferents of the rat claustrum. *Anatomy and embryology*, 173(3), pp.401–11.

Sloniewski, P., Usunoff, K.G. & Pilgrim, C., 1985. Efferent connections of the claustrum to the posterior thalamic and pretectal region in the rat. *Neuroscience letters*, 60(2), pp.195–9.

Smith, J.B., Radhakrishnan, H. & Alloway, K.D., 2012. Rat claustrum coordinates but does not integrate somatosensory and motor cortical information. *The Journal of neuroscience : the official journal of the Society for Neuroscience*, 32(25), pp.8583–8.

Smythies, J.R., Edelstein, L.R. & Ramachandran, V.S., 2014. *Hypotheses Relating to the Function of the Claustrum* J. R. Smythies, L. R. Edelstein, & V. S. Ramachandran, eds., Academic Press.

Smythies, J.R., Edelstein, L.R. & Ramachandran, V.S., 2012a. Hypotheses relating to the function of the claustrum. *Frontiers in integrative neuroscience*, 6, Article 53.

Smythies, J.R., Edelstein, L.R. & Ramachandran, V.S., 2012b. The Functional Anatomy of the Claustrum: The Net That Binds. *WebmedCentral Neuroscience*, 3(3), p.WMC003182.

Spector, I., Hassmannova, J. & Albe-Fessard, D., 1974. Sensory properties of single neurons of cat's claustrum. *Brain Research*, 66(1), pp.39–65.

Srinivas, M. et al., 1999. Functional properties of channels formed by the neuronal gap junction protein connexin36. *The Journal of neuroscience : the official journal of the Society for Neuroscience*, 19(22), pp.9848–55.

Stiefel, K.M., Merrifield, A. & Holcombe, A.O., 2014. The claustrum's proposed role in consciousness is supported by the effect and target localization of Salvia divinorum. *Frontiers in integrative neuroscience*, 8, Article 20.

Sutor, B. & Hagerty, T., 2005. Involvement of gap junctions in the development of the neocortex. *Biochimica et biophysica acta*, 1719(1-2), pp.59–68.

Söhl, G., Maxeiner, S. & Willecke, K., 2005. Expression and functions of neuronal gap junctions. *Nature reviews. Neuroscience*, 6(3), pp.191–200.

Talaverón, R. et al., 2014. Implanted neural progenitor cells regulate glial reaction to brain injury and establish gap junctions with host glial cells. *Glia*, 62(4), pp.623–38.

Tanne-Gariepy, J., Boussaoud, D. & Rouiller, E.M., 2002. Projections of the claustrum to the primary motor, premotor, and prefrontal cortices in the macaque monkey. *The Journal of Comparative Neurology*, 454(2), pp.140–157.

Traub, R.D. et al., 2003. Contrasting roles of axonal (pyramidal cell) and dendritic (interneuron) electrical coupling in the generation of neuronal network oscillations. *Proceedings of the National Academy of Sciences of the United States of America*, 100(3), pp.1370–4.

Traub, R.D. et al., 2001. Gap junctions between interneuron dendrites can enhance synchrony of gamma oscillations in distributed networks. *The Journal of neuroscience : the official journal of the Society for Neuroscience*, 21(23), pp.9478–86.

Vertes, R.P., 2004. Differential projections of the infralimbic and prelimbic cortex in the rat. *Synapse (New York, N.Y.)*, 51(1), pp.32–58.

Vervaeke, K. et al., 2010. Rapid desynchronization of an electrically coupled interneuron network with sparse excitatory synaptic input. *Neuron*, 67(3), pp.435–51.

Wang, Y., 2013. *Turnover rate of the neuronal connexin 36 in HeLa cells*. Unpublished master's thesis. University of Texas.

Wang, Y., Barakat, A. & Zhou, H., 2010. Electrotonic coupling between pyramidal neurons in the neocortex. *PloS one*, 5(4), p.e10253.

Van der Want, J.J. et al., 1998. Dendro-dendritic connections between motoneurons in the rat spinal cord: an electron microscopic investigation. *Brain research*, 779(1-2), pp.342–5.

Wasilewska, B. & Najdzion, J., 2001. Types of neurons of the claustrum in the rabbit--Nissl, Klüver-Barrera and Golgi studies. *Folia morphologica*, 60(1), pp.41–5.

Weller, R.E., Steele, G.E. & Kaas, J.H., 2002. Pulvinar and other subcortical connections of dorsolateral visual cortex in monkeys. *The Journal of comparative neurology*, 450(3), pp.215–40.

Wilhite, B.L., Teyler, T.J. & Hendricks, C., 1986. Functional relations of the rodent claustral-entorhinal-hippocampal system. *Brain research*, 365(1), pp.54–60.

Witter, M.P. et al., 1988. Reciprocal connections of the insular and piriform claustrum with limbic cortex: an anatomical study in the cat. *Neuroscience*, 24(2), pp.519–39.

Wójcik, S. et al., 2004. Analysis of calcium binding protein immunoreactivity in the claustrum and the endopiriform nucleus of the rabbit. *Acta neurobiologiae experimentalis*, 64(4), pp.449–60.

Zhang, X. et al., 2001. Susceptibility to kindling and neuronal connections of the anterior claustrum. *The Journal of neuroscience : the official journal of the Society for Neuroscience*, 21(10), pp.3674–87.

Appendix I: Figures for polyclonal rabbit anti-connexin 36 antibody tests

Abbreviations used in figures below:

CA1	-	Cornu Ammonis 1
DCW	-	Deep cerebral white matter
DG	-	Dentate gyrus
M1	-	Primary motor cortex
M2	-	Secondary motor cortex
PPC	-	Posterior parietal cortex
S1	-	Primary somatosensory cortex
TeA	-	Temporal association area
V2	-	Secondary visual cortex

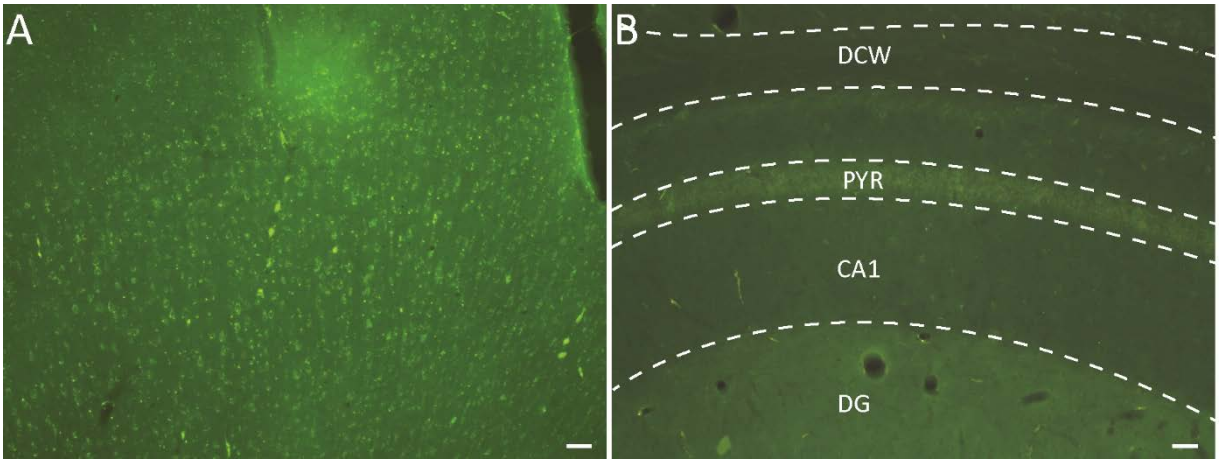

Figure I: A: Example of auto-fluorescent signal in M2 before adapting a new perfusion protocol. B: Test with 16 hours primary antibody incubation, showing absence of labeling in CA1. Scale bars: 50µm.

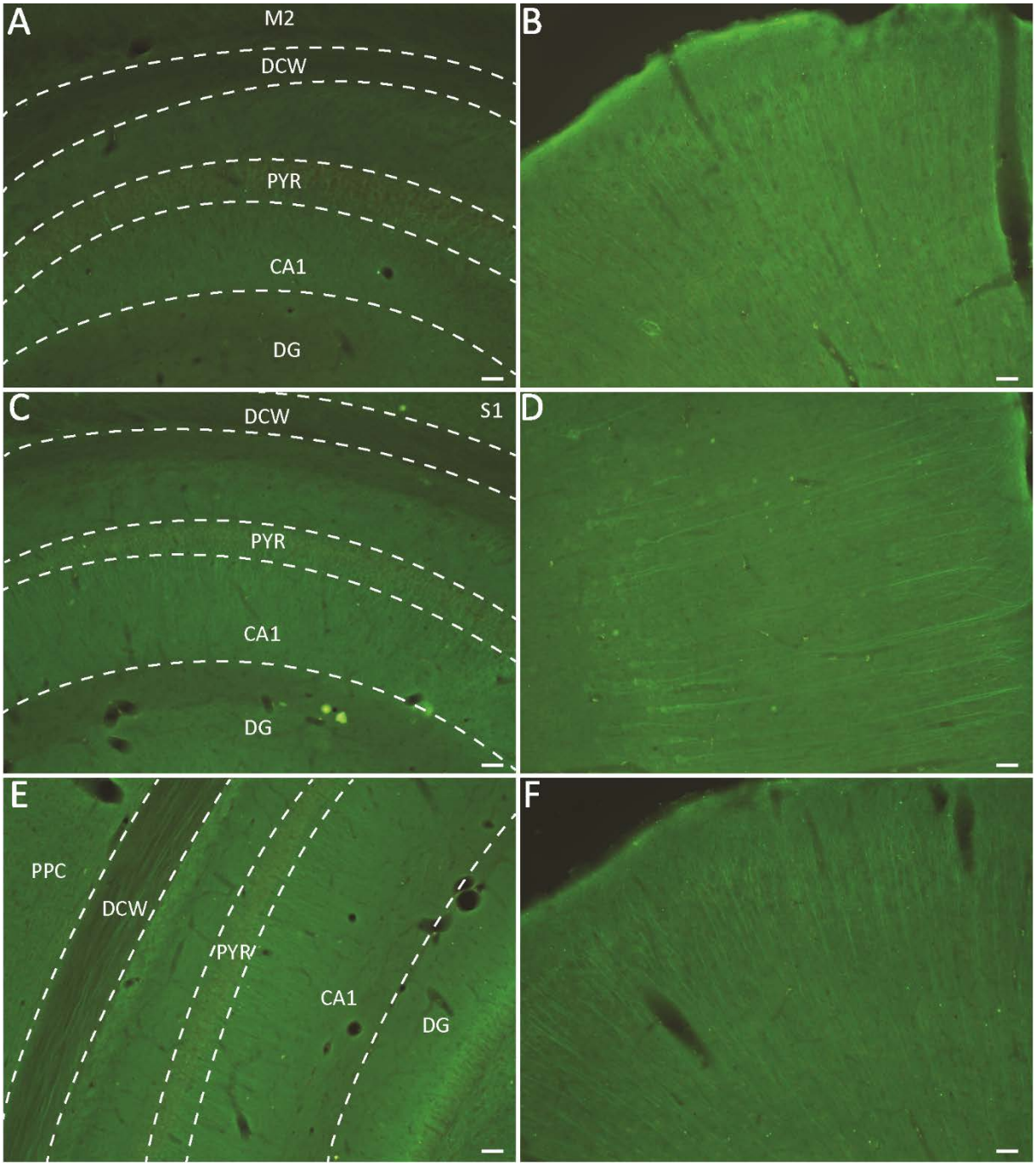

Figure II: A, B: Test with 24 hours primary antibody incubation. C, D: Test with 48 hours primary antibody incubation. E, F: Test with 1:250 primary antibody concentration. A, C, E: Specific labeling in CA1. B, D, F: Unspecific labeling in different levels of S1. Scale bars: 50µm.

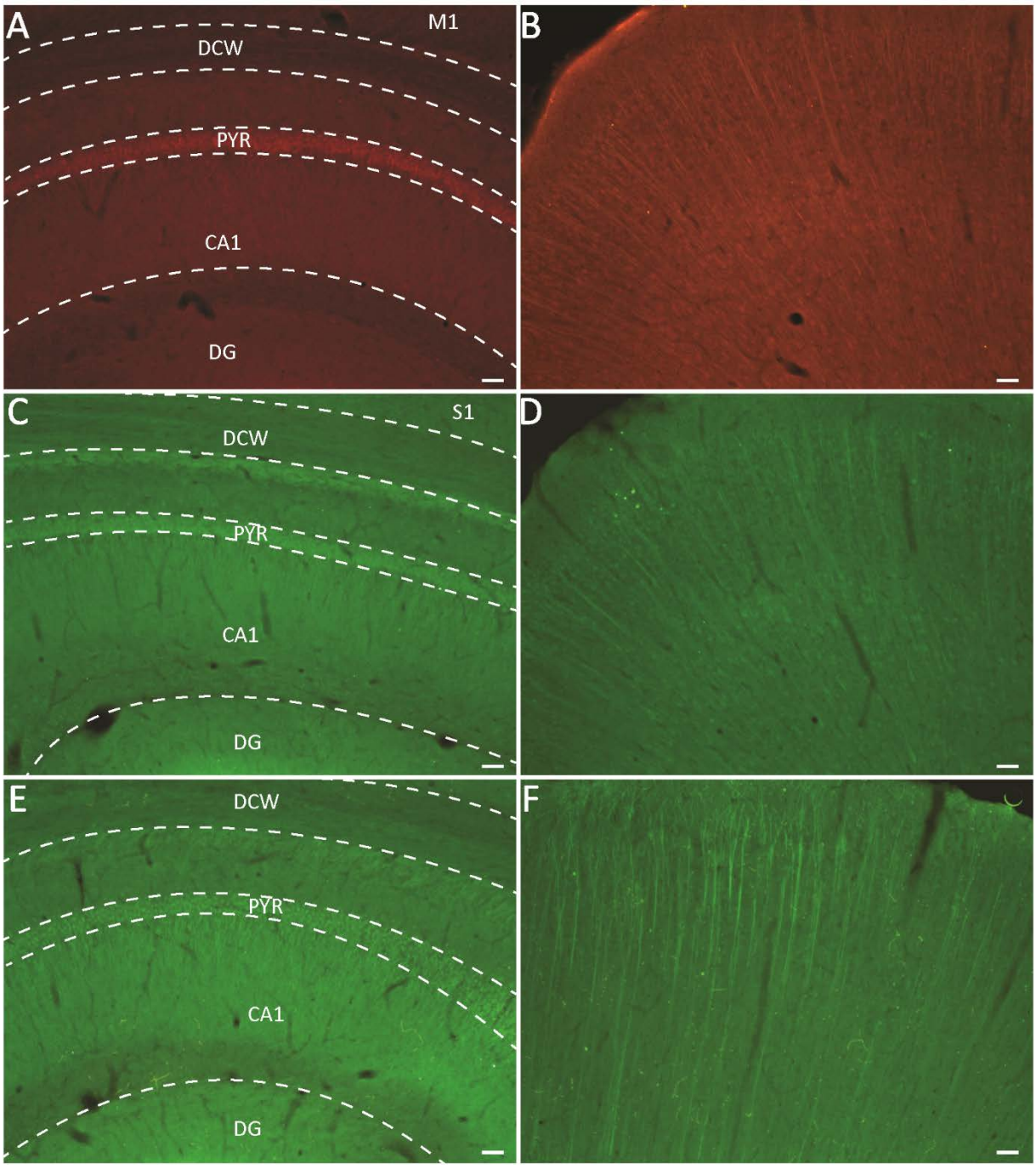

Figure III: A, B: Test with Cy3 conjugated secondary antibody. C, D: Test with one hour blocking with 5% normal goat serum. E, F: Test with heated tissue. A, C, E: Specific labeling in CA1. B, D, F: Unspecific labeling in M2(B,D) and M1(F). Scale bars: 50µm.

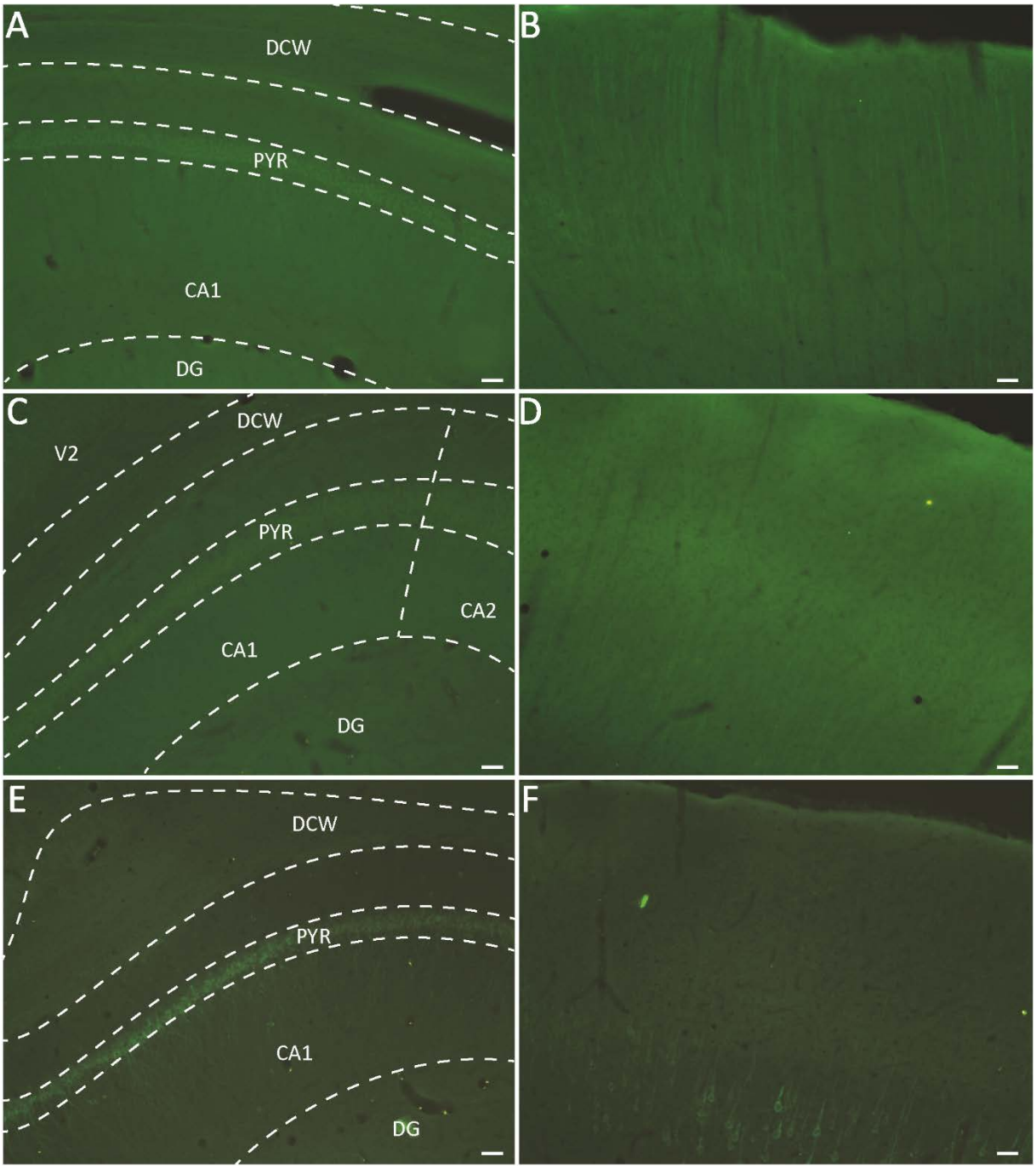

Figure IV: A, B: Test with new perfusion protocol. C, D: Test with 5% normal goat serum added to primary antibody incubation. E-F: Test tissue cut at 20µm. A, C, E: Specific labeling in CA1. B, D, F: Unspecific labeling in M1(B,F) and S1(D). Scale bars: 50µm.

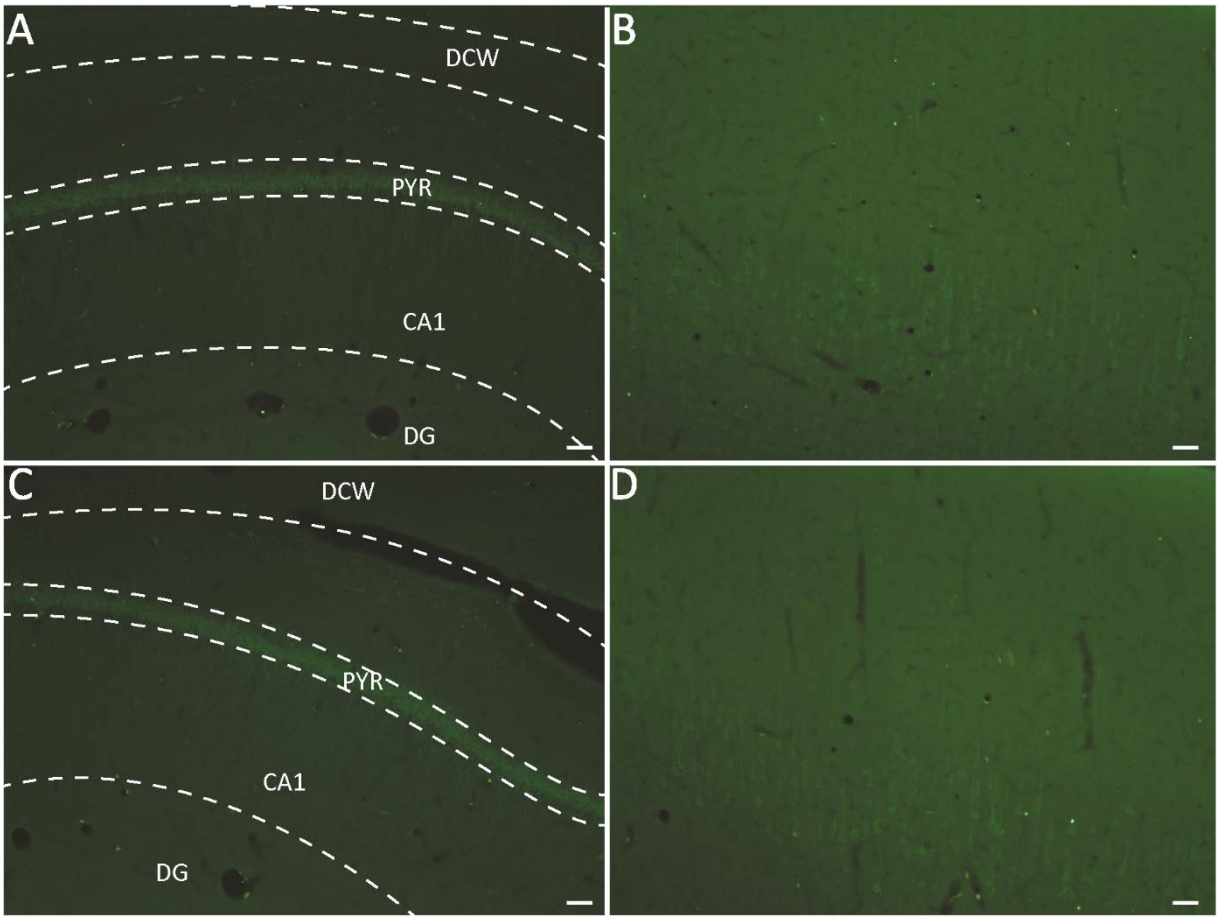

Figure V: A, B: Test with saponin permeabilization (0.1% concentration). C, D: Test with saponin permeabilization (0.4% concentration). A, C: Specific labeling in CA1. B, D: Unspecific labeling in M1. Scale bars: 50µm.

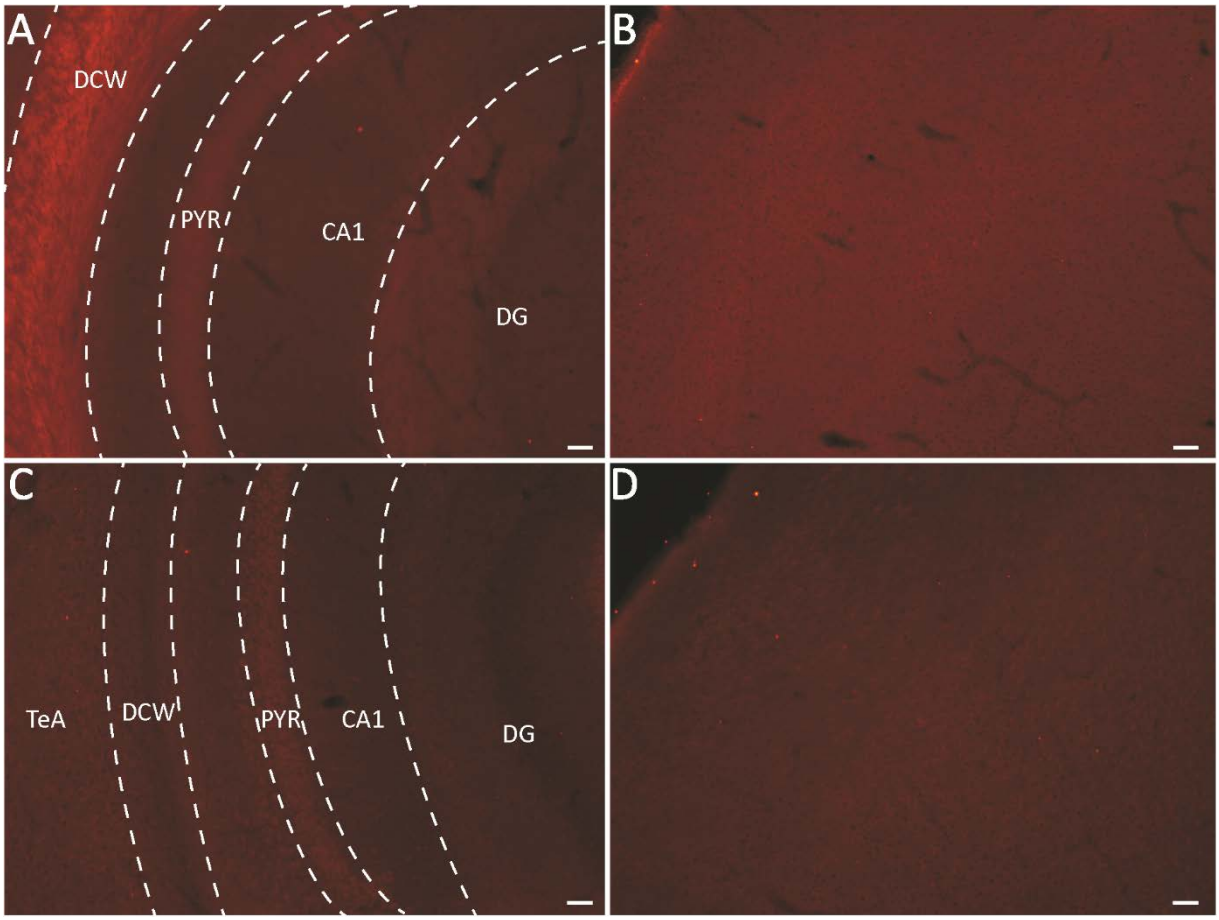

Figure VI: Test with GAD67-eGFP positive mouse. A, B: Test with 1:500 primary antibody concentration showing very weak labeling in CA1 and no labeling in S1. C, D: Test with 1:1000 primary antibody concentration showing almost no labeling in CA1 and no labeling in S1. Scale bars: 50µm.

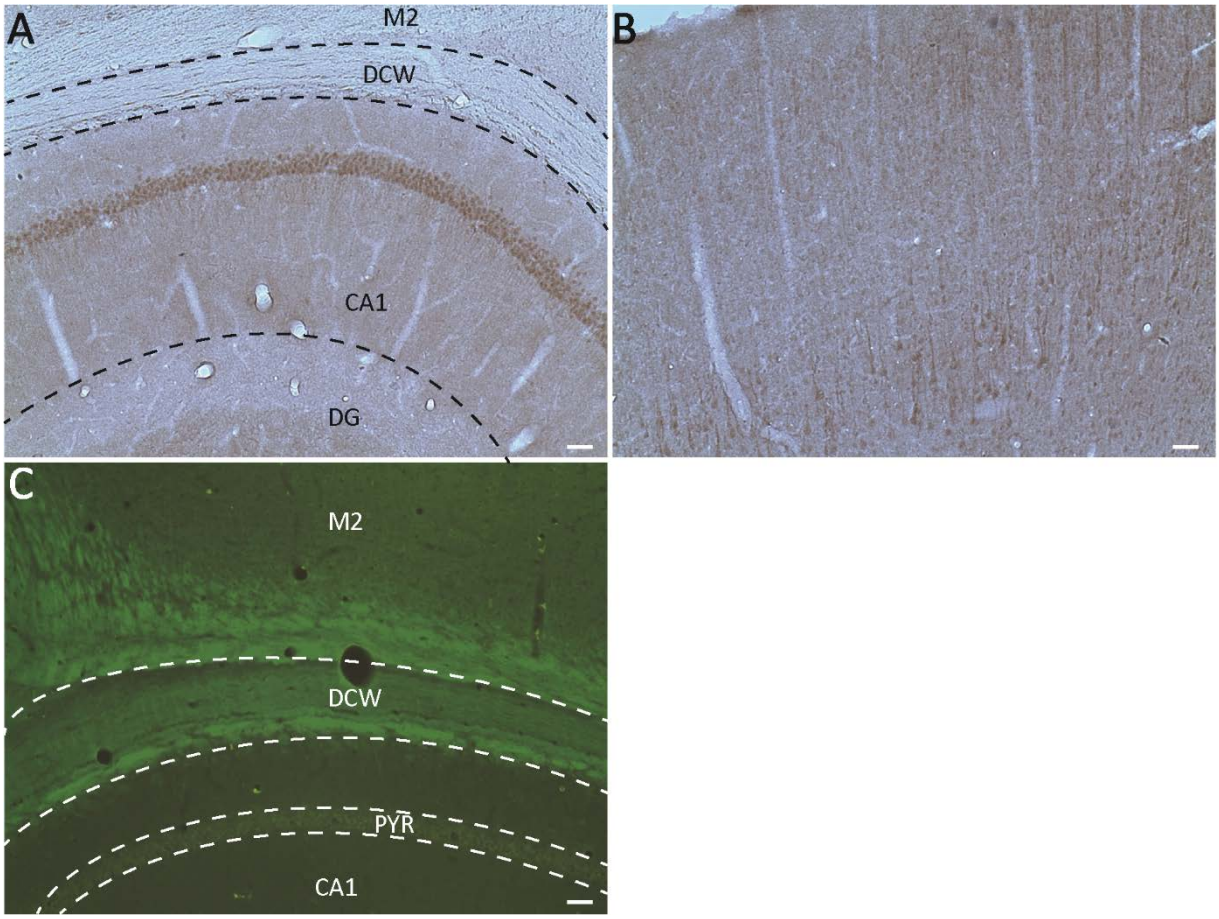

Figure VII: A: Test with DAB, showing specific labeling in CA1. B: Test with DAB, showing unspecific labeling in M1. C: Test with new batch of primary antibody, showing unspecific staining of white matter. Scale bars: 50µm.

Appendix IV: Additional electron micrographs of putative gap junctions in the Clv

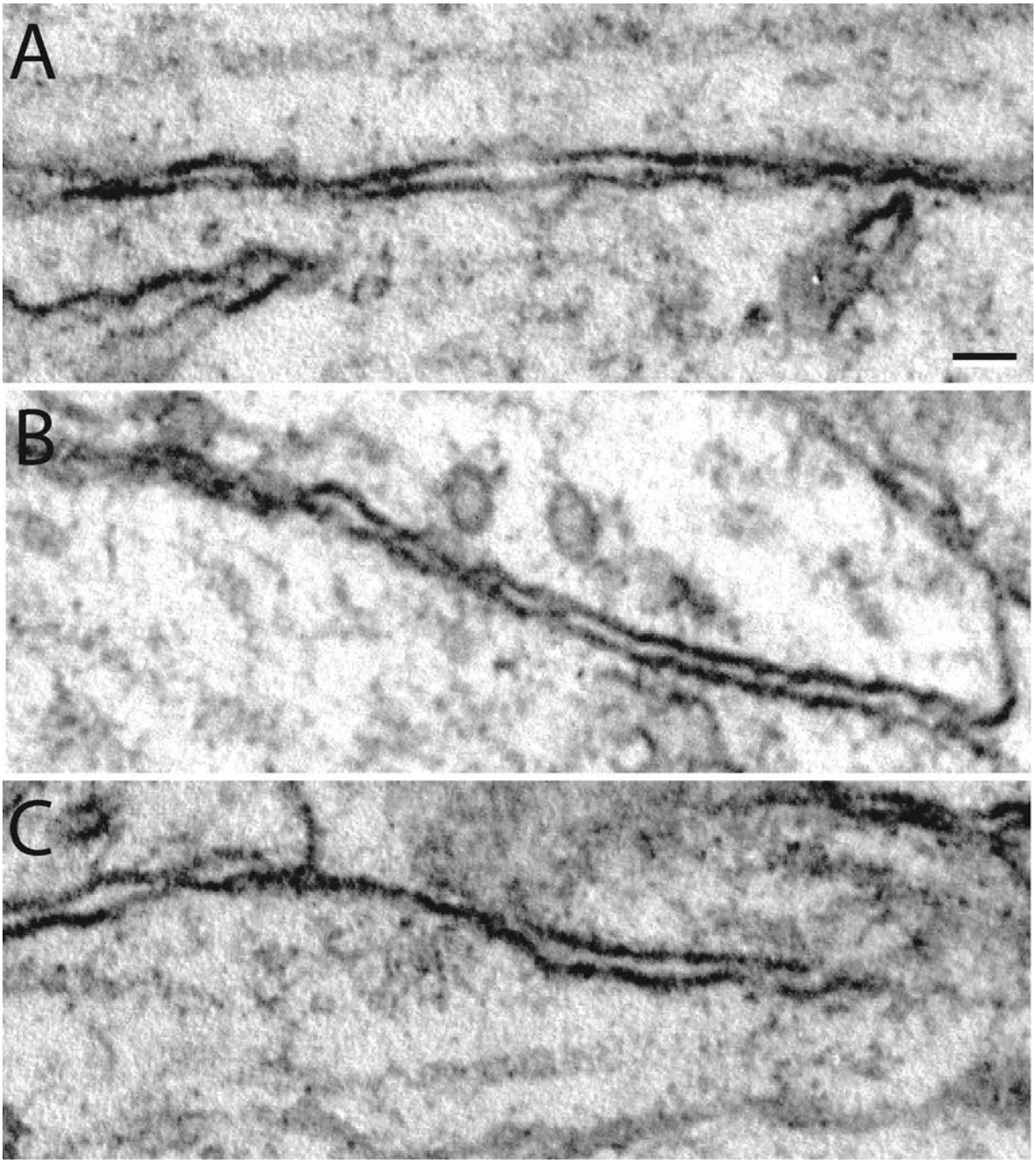

Figure VIII: Region 1 showing putative GJs between various membrane pairs found in the Clv. Scale bar: 50nm.

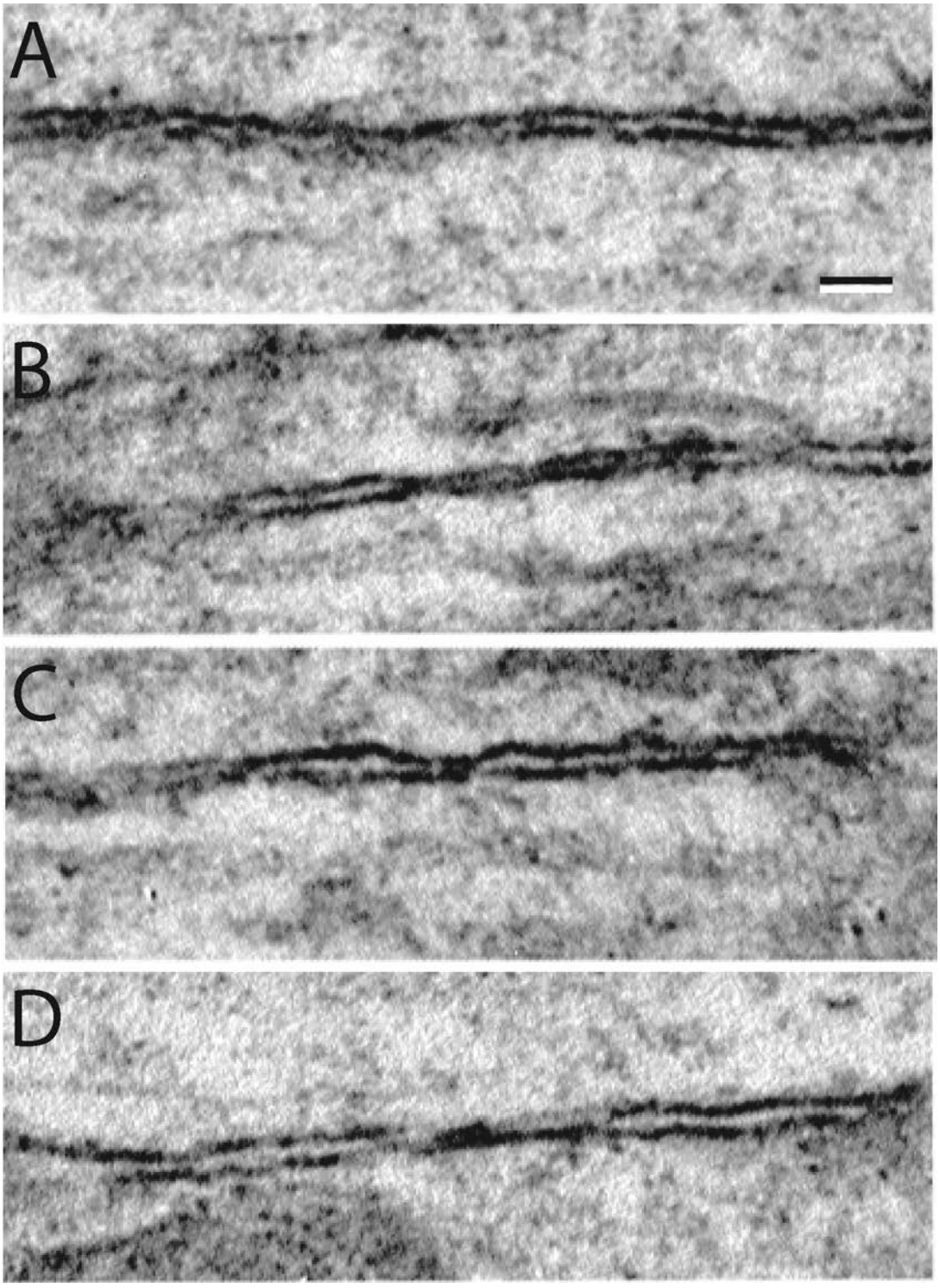

Figure IX: Region 2 showing putative GJs between various membrane pairs found in the Clv. Scale bar: 50nm.

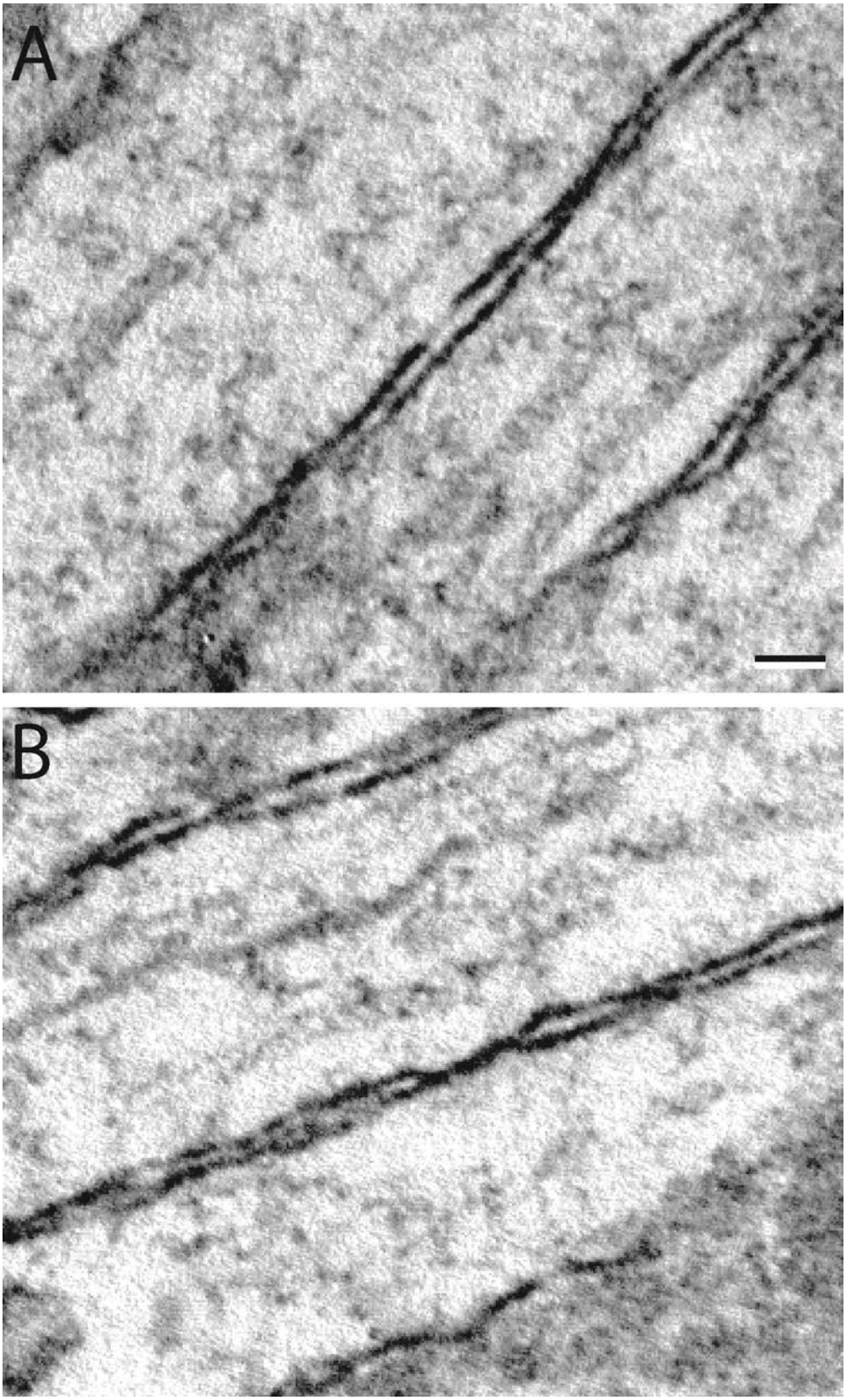

Figure X: Region 3 showing putative GJs between various membrane pairs found in the Clv. Scale bar: 50nm.

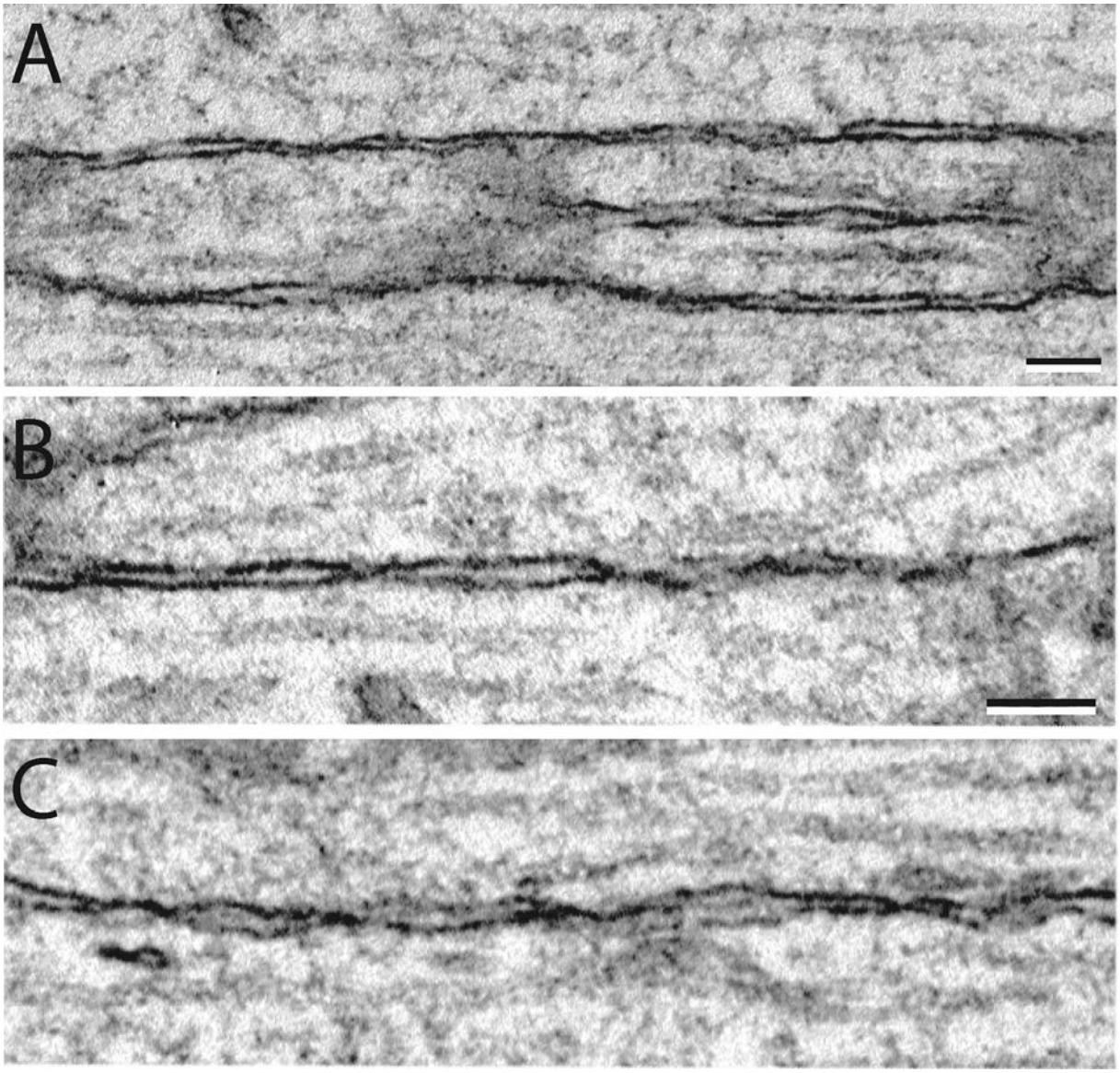

Figure XI: Region 4 showing putative GJs between various membrane pairs found in the Clv. Scale bar: A: 100nm. B-C: 100nm.

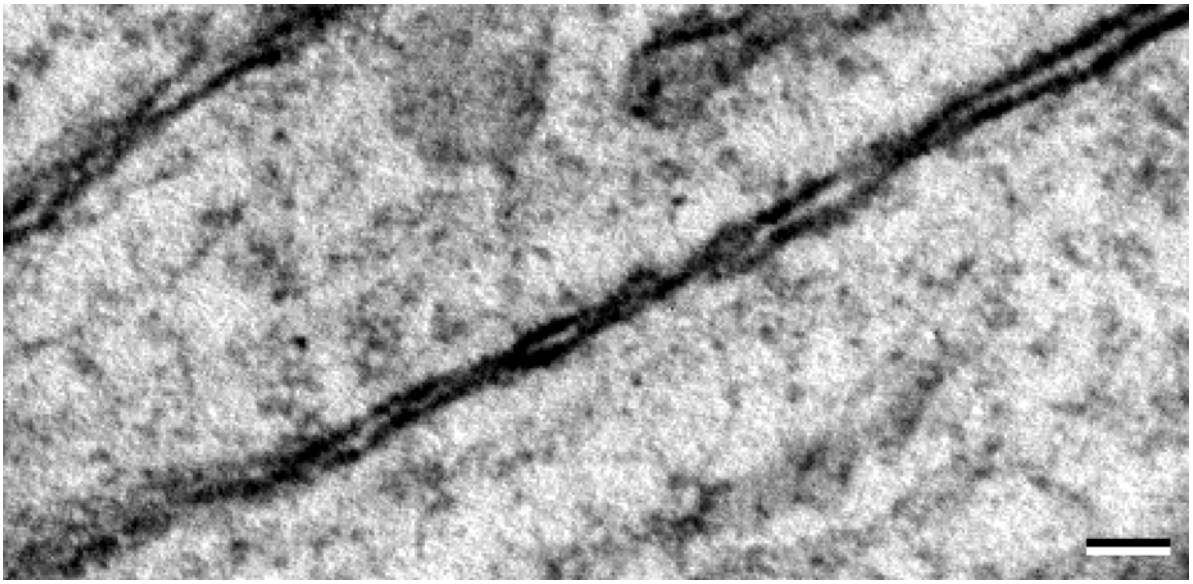

Figure XII: Region 5 showing putative GJs between various membrane pairs found in the Clv. Scale bar: 50nm.

Appendix III: Protocols for immunohistochemistry

See appendix IV for recipes of all solutions used in the protocols described here.

Immunofluorescence

1. Rinse sections 3 x 10 min in 0,125M phosphate buffer
2. Rinse 3 x 10 min in TBS-Tx
3. 1 hour in TBS-Tx + 5% Goat serum
4. Incubate for 24 hours at 4°C with primary antibody diluted 1:500 in TBS-Tx
5. Rinse 3 x 10 min in TBS-Tx
6. Incubate with secondary antibody diluted 1:400 in TBS-Tx for 90 minutes at room temperature
7. Rinse 2 x 5 min in Tris-HCl
8. Mount sections in gelatin and let them dry
9. Coverslip sections with toluene

Tissue embedding for EM

All dehydration and embedding is performed in room temperature

1. Wash 2x10 minutes in 0,1 M cacodylate buffer
2. Postfix in 0,5 ml 1% Osmiumtetroxide/1,5% potassiumferrocyanide in cacodylate, (1:1) for 15 min
3. Wash 2x5 minutes in 0,1 M Cacodylat buffer
4. 15 min in 50%, 70% and 90% Ethanol
5. 4x 20 minutes in absolute Ethanol

All the steps including Propyleneoxide are done with cap on the glasses

6. 2x20 minutes in Propyleneoxide
7. 1:3 Epoxy (LX110): Propyleneoxide for 2 hours on a rotator
8. 1:1 Epoxy (LX110): Propyleneoxide for 2 hours on a rotator
9. 3:1 Epoxy (LX110): Propyleneoxide overnight on a rotator
10. Pure epoxy (Lx110), for at least 5 hours on a rotator
11. Flat embed the tissue between two sheets of removable plastic (Aclar, or a plastic file)
12. Polymerize in at least 60°C overnight and make a flat labelled epoxy-block at the same time.
13. Remove Aclar/plastic file, and cut out the area of interest with a scalpel/razor blade
14. Glue the tissue piece on the epoxy-block with some epoxy. Make sure the tissue is flat.
15. Cure for 2 – 3 more nights at 60°C.

Grid staining for EM

1. Measure UA and lead citrate in Eppendorf tubes. Stain 1-6 grids per round (0.3 to 0.75 ml of solution).
2. Sentrifuge at 10,000 RPM for 10 min. Remember to balance the centrifuge.
3. Add Parafilm to both of the Petri dishes.
4. Pipette gently UA solution, one drop for each grid on the Parafilm.
5. Take the grids out of the grid box with a pair of tweezers.
6. Place a grid on each drop, with section side down on the drop, and put on the metal lid.
7. Stain for 10 minutes.
8. Rinse wash dishes with distilled water before use.
9. Wash the grids by rotate/dipping/for 10 times in each of the 4 baths of distilled water.
10. Wipe the grids and tweezers with filter paper.
11. Pipette gently Lead citrate solution, one drop for each grid on the Parafilm.
12. Place a grid on every drop of Lead citrate, with section side down on the drop.
13. Stain for 1,5 minutes.
14. Rinse in the meanwhile the dishes in distilled water, 2 times.
15. Wash the grids by rotate/dipping/for 10 times in each of the 4 baths of distilled water.
16. Wipe the grid and tweezers with filter paper.
17. Wait until the grids are dry before microscopy (about 1 hour).

DAB

1. Rinse sections 3 x 10 min in 0,125M phosphate buffer
2. Rinse 3 x 10 min in TBS-Tx
3. 1 hour in TBS-Tx + 5% Goat serum
4. Incubate for 24 hours at 4°C with primary antibody diluted 1:500 in TBS-Tx
5. Rinse 3 x 10 min in TBS-Tx
6. Incubate with secondary antibody (biotinylated) diluted 1:200 in TBS-Tx for 90 minutes in room temperature
7. Rinse sections 3 x 10 min in TBS-Tx
8. Incubate with ABC for 90 minutes at room temperature
9. Rinse 3 x 10 min in TBS-Tx
10. Rinse 2 x 5 min in Tris-HCl
11. Incubate with DAB until sections look dark enough
12. Rinse 2 x 5 min in Tris-HCl
13. Mount sections in gelatin and let them dry
14. Coverslip sections with toluene

Appendix IV: Recipes for solutions

See appendix V for the manufacturers of the chemicals used in the solutions described here.

Ringer (250mL):
250ml H_2O
2.125g NaCl
0.0625gKCl
0.05g $NaHCO_3$
Filtrate. Cool down to about 4°C. Use O_2 to adjust the pH to 6.9.
Make fresh ringer before every perfusion.

10% Paraformaldehyde solution (100ml):
100ml H_2O (60°C)
10g paraformaldehyde
Add a drop of NaOH and leave the solution on a hot stirrer until the solution is clear.

4% Paraformaldehyde solution (250 ml):
100ml 10% paraformaldehyde
78ml 0.4M phosphate buffer
72ml H_2O
For electron microscopy: add 3ml (0.3%) of 25% glutaraldehyde.
Use HCl to adjust the pH to 7.4. Filtrate. Cool down to 4°C.
Make new fixative for every perfusion.

2% Glutaraldehyde solution (100ml):
100ml 0.125M phosphate buffer
8ml 25% glutaraldehyde

Phosphate buffer 0.4M:
A:
500ml H_2O
27.6g $NaH_2PO_4H_2O$
B:
500ml H_2O
35.6g $Na_2HPO_4H_2O$
Make solutions A and B. Add solution A to solution B until the pH is 7.4 (= 0.4M).
Store in the dark in room temperature for up to one month.

Phosphate buffer 0.125M (100ml):
31.25 mL 0.4M phosphate buffer
68.75 mL H_2O
Store in refrigerator up to one week.

0.5% TBS-TX buffer (500ml):
500ml H_2O
3.03g Tris
4.48g NaCl
2.5ml Triton-X-100
Use HCl to adjust the pH to 8.0.
Store in refrigerator for up to one week.

0.1/0.4% Saponin buffer (500ml):
500ml H_2O
3.03g Tris
4.48g NaCl
0.5/2g Saponin
Use HCl to adjust the pH to 8.0.
Store in refrigerator for up to one week.

Tris-HCl solution (500ml):
500ml H_2O
3.03g Tris
Use HCl to adjust the pH to 7.6.
Store in refrigerator for up to one week.

Gelatin solution (100ml):
100ml Tris-HCl solution (60°C)
0.2g gelatin
Store in refrigerator for up to one week.

Sucrose solution (100ml):
100ml 0.125M phosphate buffer
30g sucrose

Cryoprotective Solution (100ml):
31.25ml 0.4M phosphate buffer
46.75ml H_2O
20ml glycerine
2ml dimethyl sulphoxide

ABC (5ml):
From the ABC-kit, put 1 drop of solution A and 1 drop of solution B in 5ml TBS-TX. Mix well and leave on the bench for 30 min before use.

DAB (15ml):
Dissolve 1 tablet (10 mg) in 15 ml Tris-HCl by leaving it on a stirrer at 50˚C (maximum) for 2 hours. Add 12 µL H_2O_2 just before use and filtrate.

Cacodylate buffer 0.2M (500ml):

21.4g Cacodylate buffer powder
500ml H_2O

Dissolve cacodylate buffer powder in 400ml water, adjust pH with NaOH to 7.4. Add 100ml water.

EM Post fixative (1% Osmiumtetroxide & 1,5% potassium ferrocyanide in cacodylate buffer):

Step 1 (Solution 1):
0.6g potassium ferrocyanide
20ml 0.2M cacodylate buffer

Step 2 (Solution 2):
1g Osmium
25ml H_2O
Stir over night
Add 25ml H_2O

Step 3:
Mix 250µl of solution 1 with 200µl of solution 2

Appendix V: List of Antibodies, chemicals and suppliers

Antibody:	Manufacturer:
Donkey anti-rabbit Cy3	Millipore
Goat anti-mouse Alexa 488	Invitrogen
Goat anti-rabbit Alexa 488	Invitrogen
Goat anti-rabbit Alexa 546	Invitrogen
Mouse anti-connexin 36	Invitrogen
Rabbit anti-connexin 36	Invitrogen
Rabbit anti-green fluorescent protein	Invitrogen

Chemicals:	Manufacturer:
1,2-Propylene oxide	Merck
3,3'-Diaminobenzidin tetrahydrochloride	Sigma-Aldrich
ABC-kit	Vector Laboratories
Cacodylic acid sodium salt	Fluka AG
Dimethyl sulphoxide	VWR
Entellan	VWR
Epoxy resin LX-112	EMS
Gelatin	VWR
Glutaraldehyde	VWR
Glycerin	VWR
Hydrogen peroxide	Sigma-Aldrich
Hydrogen chloride	Merck
Potassium chloride	VWR
Lead citrate	EMS
$Na_2HPO_4H_2O$	VWR
NaCl	VWR
$NaH_2PO_4H_2O$	Merck
Sodium bicarbonate	VWR
Sodium hydroxide	VWR
Osmium tretraoxide	EMS
Paraformaldehyde	VWR
potassium ferrocyanide	Sigma-Aldrich
Saponin	VWR
Sucrose	VWR
Toluene	VWR
Tris	VWR
Triton-X-100	VWR
Uranyl acetat	SPI Supplies